Progress in Oceanography xxx (2014) xxx–xxx

Contents lists available at ScienceDirect

Progress in Oceanography

journal homepage: www.elsevier.com/locate/pocean

Meridional overturning transports at 7.5N and 24.5N in the Atlantic Ocean during 1992–93 and 2010–11

Alonso Hernández-Guerra [a,*], Josep L. Pelegrí [b], Eugenio Fraile-Nuez [c], Verónica Benítez-Barrios [c], Mikhail Emelianov [b], María Dolores Pérez-Hernández [a], Pedro Vélez-Belchí [c]

[a] Instituto de Oceanografía y Cambio Global (IOCAG), Universidad de Las Palmas de Gran Canaria, 35017 Las Palmas, Spain
[b] Department d'Oceanografía Física i Tecnològica, Institut de Ciències del Mar, CSIC, Passeig Marítim de la Barceloneta 37-49, 08003 Barcelona, Spain
[c] Instituto Español de Oceanografía, Centro Oceanográfico de Canarias, 38180 Santa Cruz de Tenerife, Spain

ARTICLE INFO

Article history:
Received 13 March 2014
Received in revised form 26 August 2014
Accepted 31 August 2014
Available online xxxx

ABSTRACT

Transatlantic hydrographic sections along latitudes 7.5N and 24.5N have been repeated with about 20 years difference, at the beginning of the 1990s and 2010s. For each period, an inverse model is applied to the closed box bound by both sections. The model imposes mass conservation for individual layers, defined by isoneutral surfaces, and the whole water column, using surface Ekman transport and several transport constraints for specific ranges of longitudes and depths. As a result, the velocities at the reference layer for each station pair and the dianeutral velocities between layers are estimated, and the horizontal velocity fields and the water, heat and freshwater transports are calculated; in particular, we find that mass transport per stratum at 24.5N in 2011 is in good agreement with the transport estimates from the RAPID-Watch array. During both realizations the dianeutral velocities downwell from the Upper North Atlantic Deep Water (UNADW) to the Lower North Atlantic Deep Water (LNADW) strata, resulting in the merging of the two southward flowing strata at 24.5N into one deep southward-moving stratum at 7.5N. At 24.5N, there is an increase in southward UNADW transport between 1992 and 2011, compensated by a decrease of southward LNADW transport; a descent in the upper limit of the Antarctic Bottom Water (AABW) from 1992 to 2011 is also inferred. The Atlantic Meridional Overturning Circulation (AMOC) is larger in 1992–93 than in 2010–11, decreasing from 24.7 ± 1.7 to 20.1 ± 1.4 Sv at 24.5N and from 29.2 ± 1.7 to 16.9 ± 1.5 Sv at 7.5N. Much of this decrease arises because of the northward flow of Antarctic Intermediate Water (AAIW), which was much more intense in 1992–93 than in 2010–11. As a consequence, heat transport at 24.5N is not significantly different in 1992 (1.4 ± 0.1 PW) and 2011 (1.2 ± 0.1 PW). The estimation of heat transport at 7.5N strongly depends on the magnitude of the North Brazil Current over the American continental platform. The freshwater flux into the box bounded by the two transoceanic sections decreases significantly from 1992–93 (−0.45 ± 0.05 Sv) to 2010–11 (−0.36 ± 0.3 Sv), meaning a decrease in net evaporation over this same area.

Introduction

The tropical and subtropical North Atlantic Oceans play an important role in the global ocean circulation. The Atlantic Meridional Overturning Circulation (AMOC) transports cold North Atlantic water masses to the south, mainly along the Deep Western Boundary Current (DWBC). In the southern and tropical Atlantic these water masses interact with waters originated around the continental shelf of Antarctica. The returning AMOC branch consists of surface and intermediate waters with relatively high temperatures (Dickson and Brown, 1994). Although the meridional water mass transport is balanced there is a net ocean transport of large amounts of heat towards northern latitudes (Ganachaud and Wunsch, 2000, 2003; Wunsch, 2005).

During the last two decades of the past century, the World Ocean Circulation Experiment (WOCE) aimed at estimating the transports of mass, heat and freshwater in every ocean. As result, a consistent picture of the ocean circulation emerged (Ganachaud and Wunsch, 2000, 2003). Several other studies compared these realizations with earlier ones, carried out for example during the International Geophysical Year (IGY), to examine decadal variations of these transports at selected latitudes (e.g., Koltermann et al., 1999; Roemmich and Wunsch, 1985).

The most surveyed transoceanic section is located in the Atlantic Ocean at 24.5N. Hydrographic sections have been carried

* Corresponding author.
E-mail address: alonso.hernandez@ulpgc.es (A. Hernández-Guerra).

http://dx.doi.org/10.1016/j.pocean.2014.08.016
0079-6611/

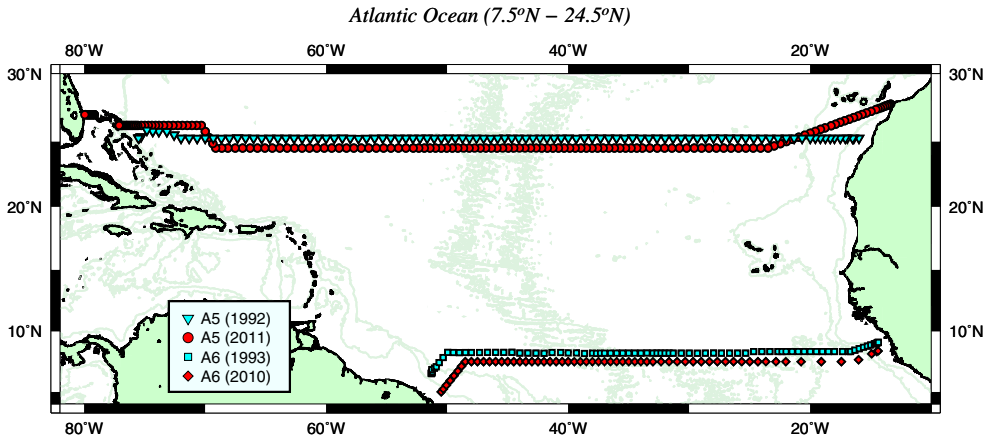

Fig. 1. Map showing the hydrographic sections carried out in 1993 and 2010 at 7.5N (section A06) and in 1992 and 2011 at 24.5N (section A05). Note that cruise tracks in 1993 at 7.5N and in 1992 at 24.5N are offset 0.5 degree in latitude for clarity.

out in 1957 in the frame of the IGY (Fuglister, 1960), in 1981 (Roemmich and Wunsch, 1985), in 1992 and 1998 in the frame of the WOCE (Baringer and Molinari, 1999; Parrilla et al., 1994), in 2004 (Bryden et al., 2005a,b), in 2010 (Atkinson et al., 2012), and in 2011 under the Malaspina project. The section at 7.5N in the Atlantic Ocean has been carried out three times: in 1957 as part of the IGY (Fuglister, 1960), in 1993 under the WOCE (Lux et al., 2001), and in 2010 under the MOC2 project. As part of WOCE the 7.5N and 24N transoceanic sections were respectively denoted as A06 and A05, a notation we will follow throughout this study.

A classical method used to estimate the ocean circulation within closed regions is the inverse model, first introduced in physical oceanography by Wunsch (1977) (see also Wunsch, 1996). The inverse method consists of an underestimated set of equations comprising the thermal wind equation and mass conservation. In this paper we present the results of applying the inverse model to sections 7.5N and 24.5N carried out in 1992–1993 and 2010–2011 (Fig. 1). As the same methodology is applied, any observed differences shall come only from the data. Thus, our results will be informative of the sort of changes in water-mass, heat and freshwater transports associated to AMOC between 1992–93 and 2010–11.

The paper is organized as follows. Section 'Data and verticals sections' presents the dataset, using both potential temperature (θ) – salinity (S) diagrams and vertical sections for potential temperature, salinity and neutral density, in order to identify the water masses and their distribution. Section 'Setup of the inverse box model' describes the implementation of the inverse model. Section 'Final adjusted transport' presents the circulation patterns that come out from the inverse model at 7.5N and 24.5N, and compares them with both previous estimates and the Rapid-WATCH data. Section 'Atlantic Meridional Overturning Circulation, heat and freshwater flux' summarizes the observed changes in the water mass, heat and freshwater fluxes of the AMOC. We finish in Section 'Discussion and conclusions' with a discussion and conclusions.

Data and verticals sections

Data from 1992 at 24.5N (section A05) and 1993 at 7.5N (section A06) were collected through the CLIVAR and Carbon Hydrographic Data Office (CCHDO). The corresponding data for 2010 (section A06) and 2011 (section A05) were originally part of projects MOC2 and Malaspina, the data now also being available from CCHDO. Section A05 carried out in 2011 also collected 15 hydrographic stations across the Florida Current, to be used in our study. Table 1 shows the most relevant information for each cruise. The separation between adjacent stations was typically 50 km, or less across boundary currents and topographic slopes, except between four eastern basin stations along section A06 during 2010 where the separation reached 150 km (Fig. 1). Hereafter, we will refer to the western and eastern basins as those Atlantic basins separated by the Mid-Atlantic Ridge (MAR), located approximately at 32W in the 7.5N section and 45W in the 24.5N section. There are also some small latitudinal differences between the sections, specifically in the western boundary at 7.5N and in the eastern boundary at 24.5N; in particular, section A05 carried out in 2011 has the highest spatial resolution among all transoceanic sections at this latitude, and its eastern margin followed a path similar to other recent 24.5N sections (Atkinson et al., 2012). At each station, a conductivity–temperature–depth (CTD) profile covered the full water column and water samples were collected with the rosette for sampling several properties as well as for calibrating the salinity values.

Current velocities were measured with two Acoustic Doppler Current Profiler (ADCP) systems during the 2010 and 2011 (A06 and A05) cruises. The first one consisted of a Lowered ADCP (LADCP) that sampled the water velocities throughout the whole water column. Both cruises had the dual configuration that consists of a downward and an upward looking 300 kHz LADCP mounted inside the CTD-rosette system. Unfortunately, three out of four LADCPs onboard the A05 cruise had flooding problems and only a downward looking LADCP was used. Thus, LADCP-derived velocities for section A05 are characterized by high noise levels and are not used in this study. The second one consisted in a Ship-mounted ADCP (SADCP), sampling the top 500 m of the water column with a low noise-to-signal ratio.

The θ–S diagram drawn using all 1993–2010 and 2010–2011 stations may be used to rapidly identify the presence of different water masses (Fig. 2). The vertical distributions of temperature, salinity and neutral density (γ_n) are shown for both the 1990s and 2010s realizations (without including the Florida Strait at 24.5N; Figs. 3–5). The 2010 realization for section A06 has been published in San Antolín Plaza et al. (2012) but it is plotted here together with the novel A05 cruise to ease their comparison. The 1992–1993 sections are presented in http://www-pord.ucsd.edu/whp_atlas/atlantic_index.htm.

Fig. 2 shows high scattering in the near surface potential temperature and salinity values at both 7.5N and 24.5N. The surface waters at 24.5N, in a region of high evaporation between 25W and 55W, actually reach the maximum surface salinities (>37.0) of the global ocean (Fig. 4). The near-surface variability at 24.5N arises because of the presence of waters of southern origin in the

Please cite this article in press as: Hernández-Guerra, A., et al. Meridional overturning transports at 7.5N and 24.5N in the Atlantic Ocean during 1992–93 and 2010–11. Prog. Oceanogr. (2014), http://dx.doi.org/10.1016/j.pocean.2014.08.016

Table 1
Hydrographic cruise information: 1992 and 1993 CTD data are available through the CLIVAR and Carbon Hydrographic Data Office (CCHDO) (http://cchdo.ucsd.edu); 2010 and 2011 CTD and LADCP data have been provided by the chief scientists.

	Dates	No. stations	Ship	Chief scientist
A05-1992	14 July to 15 August 1992	112	Hespérides	Gregorio Parrilla (Instituto Español de Oceanografía, Spain)
A05-2011	27 January to 15 March 2011	167	Sarmiento de Gamboa	Alonso Hernández-Guerra (Universidad de Las Palmas de Gran Canaria, Spain)
A06-1993	13 February to 19 March 1993	84	L'Atalante	Christian Colin (ORSTOM, France)
A06-2010	5 April to 16 May 2010	62	Hespérides	Josep L. Pelegrí (Institut de Ciències del Mar, Spain)

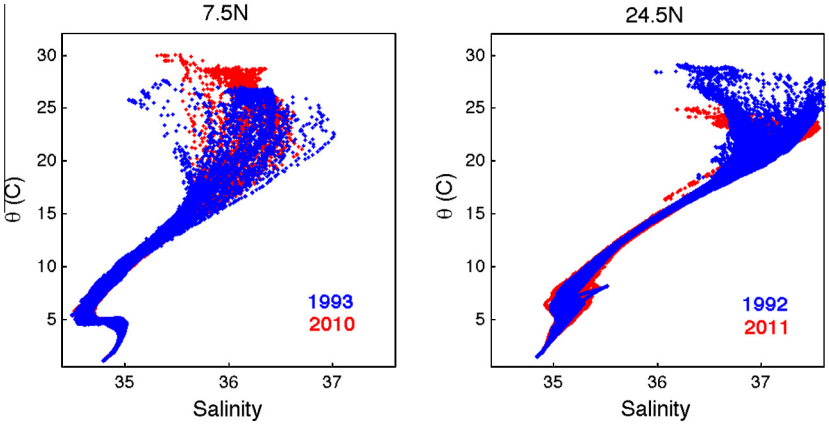

Fig. 2. θ/S diagram for 1993/2010 at 7.5N-A06 (left panel) and 1992/2011 at 24.5N-A05 (right panel).

Florida Strait (Schmitz Jr. and Richardson, 1991) and coastal upwelling in the eastern boundary (Hernández-Guerra and Nykjaer, 1997; Marcello et al., 2011; Pacheco and Hernández-Guerra, 1999). At 7.5N this variability is the result of the intrusion of warm and salty waters associated to the North Equatorial Counter Current in the western margin (Bourles et al., 1999) and the influence of the Dome of Guinea upwelling in the eastern margin (Nykjaer and Van Camp, 1994).

The permanent thermocline layer (corresponding to $\theta > 10$ °C) along 24.5N is quite deep, down to about 800/600 m in the western/eastern margins, with the property isolines rising towards the eastern basin (Figs. 2 and 3a and b); the signal of the Antilles Current is clearly seen at the western edge, with the westward rise of the isotherms, isohalines and isoneutrals. In contrast, at 7.5N the permanent thermocline is much shallower, with the 10 °C isotherm reaching only about 200 m in the western margin and 400 m in the eastern margin (Figs. 2 and 3c and d); the deepening of this isothermal at the eastern margin is a signature of a dominant first baroclinic mode associated to the Guinea Dome region (Machín and Pelegrí, 2009).

The different salinity and temperature values reflect the presence of North Atlantic Central Water (NACW) at 24.5N and South Atlantic Central Water (SACW) at 7.5N (Hernández-Guerra et al., 2005). Both SACW and NACW are characterized by a nearly linear θ–T relationship (Harvey, 1982; Tomczak and Hughes, 1980) (Fig. 2). In the salinity vertical sections the NACW displays constant slope isohalines (Fig. 4a and b) while the SACW shows a more patchy distribution (Fig. 4c and d). According to Pollard and Pu (1985) and van Aken (2001), the salinification of the whole NACW stratum is caused by winter cooling and vertical convection of saline surface waters near the west and northwest of Spain and Portugal. The boundary between the NACW and SACW in the eastern margin is located at 20–22N in the Cape Verde Frontal Zone (Martínez-Marrero et al., 2008; Pastor et al., 2012; Zenk et al., 1991). At 7.5N the equatorial 13 °C thermostad only shows up in the eastern basin (Fig. 3) (Tsuchiya et al., 1992). In contrast, at 24.5N the 18 °C thermostad only appears in the western basin (Fig. 3). The isotherms and isohalines, and as a result the isoneutrals, tilt in opposite directions along 7.5N and 24.5N, respectively reflecting the predominant cyclonic and anticyclonic large-scale circulation in the tropical and subtropical regions (Fraile-Nuez and Hernández-Guerra, 2006; Hernández-Guerra et al., 2010) (Figs. 3–5).

The θ–S diagram shows the intermediate layers (27.38kg m^{-3} < $\gamma_n \leqslant$ 27.922 kg m^{-3}, approximately in the 700–1600 m depth range) to be affected by two water masses with extreme salinity values, Antarctic Intermediate Water (AAIW) and Mediterranean Water (MW) (Fig. 2). AAIW is best observed at 7.5N, with salinities less than 34.7 centered at about 800 m, while MW brings an increase in salinity in the eastern basin at 24.5N, with maximum values in the 900–1400 m depth range (Arhan et al., 1994) (Fig. 4). The vertical section of salinity at 24.5N presents relative high mesoscale variability in the longitude range ~35–65W as higher salinity MW and lower salinity AAIW are encountered. The density ranges of these water masses at both latitudes show considerable overlap likely leading to isopycnal and diapycnal mixing (Figs. 2 and 5). A Meddy (Mediterranean Water Eddy) was found in 1992 at 24.5W, centered at about 1200 m and 27W (Fig. 4), clearly showing up in the θ–S diagram because of its high salinity content (Fig. 2); Meddies are usually found in an elliptical area southwest of Portugal (Richardson et al., 2000). The salinity of the intermediate waters in the eastern margin is significantly higher in 2011 than in 1992, likely reflecting the existence of a seasonal intrusion of low salinity waters near the African coast (Hernández-Guerra et al., 2005; Iorga and Lozier, 1999; Roemmich and Wunsch, 1985), with higher AAIW content in fall and early winter and a greater MW contribution in late winter and spring (Fraile-Nuez et al., 2010; Hernández-Guerra et al., 2003; Machín et al., 2006). This fact has been explained through the latitudinal displacements associated with the stretching and shrinking of the intermediate water strata in the tropical region (Machín and Pelegrí, 2009; Machín et al., 2010).

The North Atlantic Deep Water (NADW) appears along 7.5N and 24.5N at γ_n ranges of 27.922–28.1295 kg m^{-3}. At both latitudes the

Please cite this article in press as: Hernández-Guerra, A., et al. Meridional overturning transports at 7.5N and 24.5N in the Atlantic Ocean during 1992–93 and 2010–11. Prog. Oceanogr. (2014), http://dx.doi.org/10.1016/j.pocean.2014.08.016

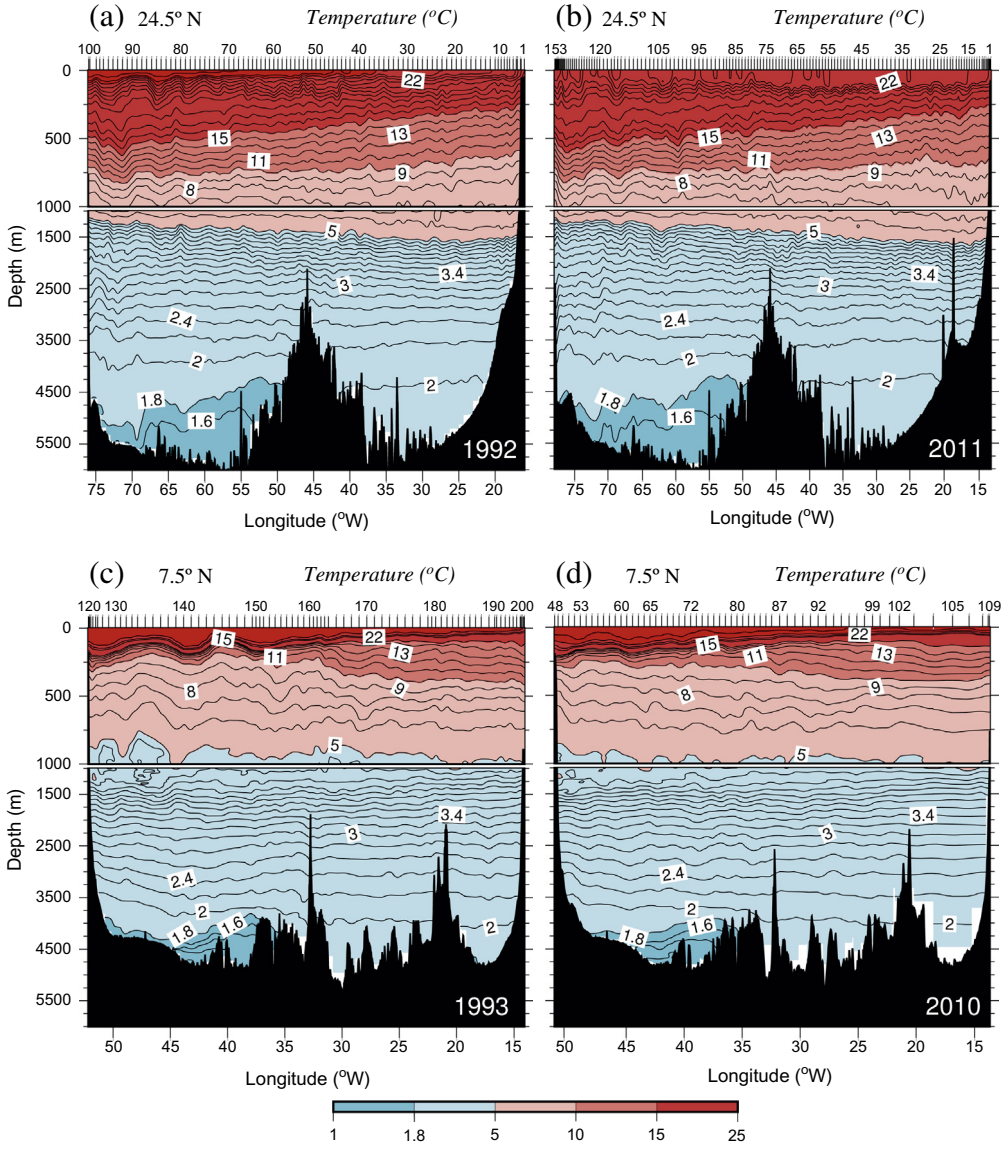

Fig. 3. Vertical sections of potential temperature (°C) along 24.5N in (a) 1992 and (b) 2011, and along 7.5N in (c) 1993 and (d) 2010.

isohalines, isotherms and isoneutrals (Figs. 3–5) are approximately flat except in the western basin where they rise reflecting the presence of the Deep Western Boundary Current (DWBC). The DWBC transports two different water masses: Upper North Atlantic Deep Water (UNADW), essentially formed by Labrador Sea waters (Talley and McCartney, 1982), and Lower North Atlantic Deep Water (LNADW), with overflow water from the Nordic Sea (Pickart, 1992; Smethie et al., 2000). At 24.5N we find the UNADW at around 1700 m and the more dense LNADW at around 4000 m (Pickart, 1992; Smethie et al., 2000). An outstanding sharp tilt of the deep western boundary isopycnals (2500–4500 m) is observed at 24.5N in 2011 (Fig. 5b). The western moorings of the Rapid-WATCH program also show this large isopycnal displacement right at the western frontier during the same days of our survey (Eleanor Frakja-Williams, personal communication).

Antarctic Bottom Water (AABW) is formed around Antarctica and flows north, as the densest waters in all oceans, along the western Atlantic basin (Johnson, 2008; Orsi et al., 1999). AABW shows up in both sections with temperature and salinity less than 1.8 °C and 34.88, at depths greater than about 4500 m (Figs. 3 and 4). An abyssal thermocline and isohaline shows up in both sections, stronger in 7.5N than in 24.5N, sloping up from the western abyssal plain towards the MAR. In the eastern basin, diluted AABW is found to progress north through the Vema Fracture Zone at 11N (McCartney et al., 1991). Temperature and salinity increases from 7.5N to 24.5N likely as a result of mixing with the overlying warmer and saltier NADW.

Setup of the inverse box model

Initial solution

The basis of our calculations is the thermal wind equation. This relation uses the density fields in two adjacent stations in order to compute the geostrophic velocities normal to the vertical plane formed by both stations, always relative to a properly selected reference level. The vertical velocity gradients do not depend on the choice of reference level but the absolute velocity values do. Therefore, the simplest model would set a reference level of no motion and calculate the geostrophic velocity field referenced to that level, neglecting any possible vertical exchange. If any of the pair of

Please cite this article in press as: Hernández-Guerra, A., et al. Meridional overturning transports at 7.5N and 24.5N in the Atlantic Ocean during 1992–93 and 2010–11. Prog. Oceanogr. (2014), http://dx.doi.org/10.1016/j.pocean.2014.08.016

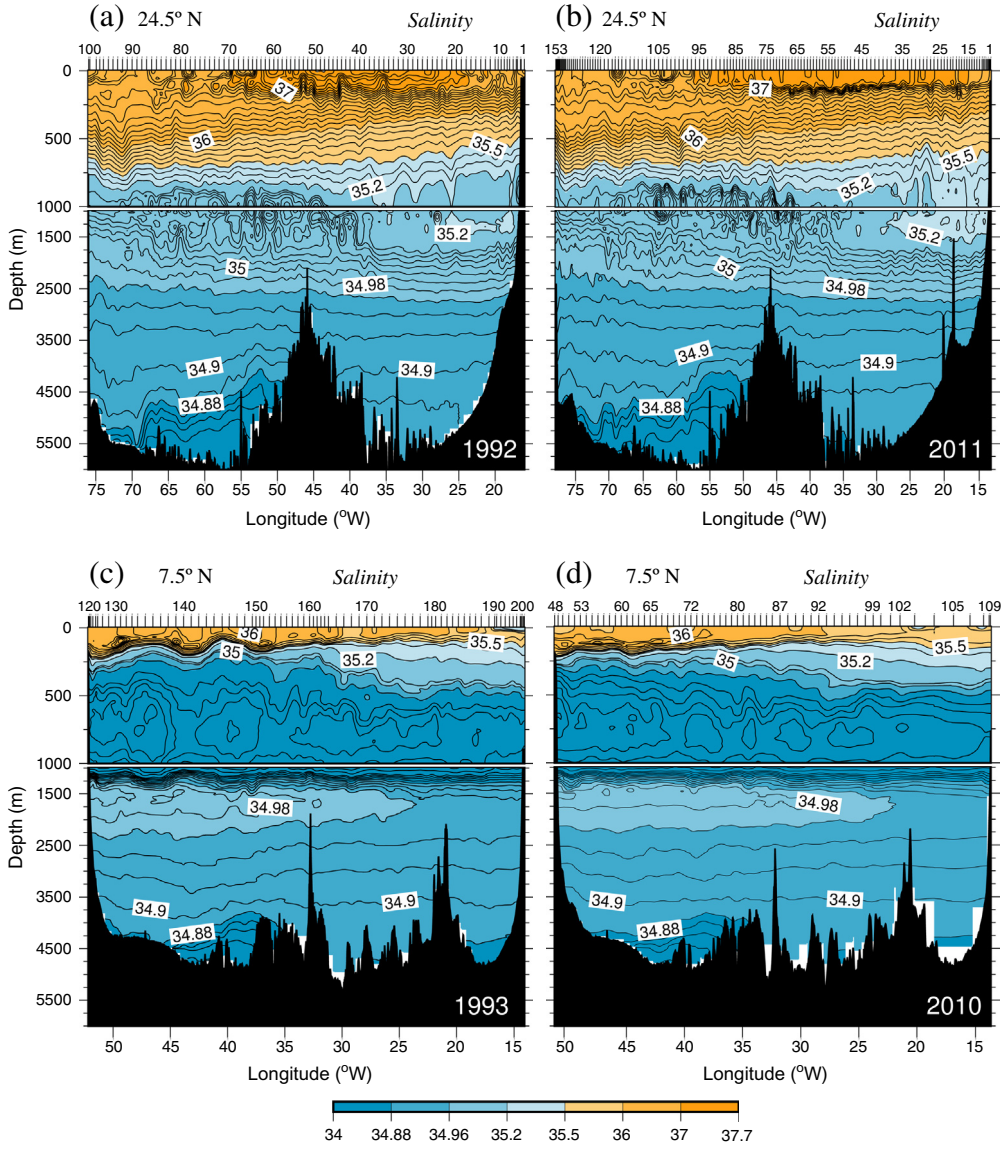

Fig. 4. Vertical sections of salinity along 24.5N in (a) 1992 and (b) 2011, and along 7.5N in (c) 1993 and (d) 2010.

stations used to calculate the geostrophic velocity is shallower than the reference layer then the deepest common level is used instead as the reference layer. In that circumstance, typically over the continental slope, the velocity in the triangular section below this level is taken to be constant and equal to the velocity at the reference level. Let us next examine this simplest case, what is to be named the initial solution.

Consider first the reference level for section A05 (along 24.5N). For the 1992 realization we have chosen the reference level as the layer defined by $\gamma_n = 28.1295$ kg m^{-3}, which separates LNADW from AABW (Ganachaud, 2003a). This neutral density isoline shows an overall rise towards the east, over the western flank of the MAR, which leads to the northward advection of the AABW. For the 2011 realization we have chosen a slightly denser and deeper layer of no motion, $\gamma_n = 28.141$ kg m^{-3}. This is because the $\gamma_n = 28.1295$ kg m^{-3} isoneutral becomes quite flat in the western margin, what would lead to null northward motions over the western abyssal plain; further, this choice would cause no southward motion of LNADW east of 30W. The implied 1992 to 2011 descent in the upper limit of the AABW is coherent with the contraction of this layer as observed by Purkey and Johnson (2012).

Let us next turn to the choice of the reference level for section A06 (along 7.5N). Following Lux et al. (2001) we let the reference layer change between different groups of stations: $\sigma_1 = 32.30$ ($\gamma_n = 27.7633$ kg m^3) for the western basin, $\sigma_4 = 45.85$ ($\gamma_n = 28.0986$ kg m^{-3}) for the western half of the eastern basin and $\sigma_4 = 45.83$ ($\gamma_n = 28.0856$ kg m^{-3}) for the eastern half of the eastern basin (Fig. 5). As a simple sensitivity study, we have explored how much the results change when setting the layer of no motion for the western half of the eastern boundary at $\gamma_n = 28.11$ kg m^{-3} and $\gamma_n = 27.7633$ kg m^{-3} instead of $\gamma_n = 28.0986$ kg m^{-3}; all cases show similar velocity patterns, with the selection of the shallower layer leading to a slightly stronger overturning circulation at 7.5N in 1993.

At 7.5N in the western boundary, the North Brazil Current (NBC) flows to the north connecting the South and North Atlantic Oceans. It is an important pathway of the returning flow of the Atlantic Meridional Overturning Circulation (AMOC) (Lumpkin and Speer, 2003). During the 2010 cruise, the transport of the NBC over the Brazil continental shelf and from the shelf break to the first station at 7.5N is directly computed from the SADCP data, and an equal value is assumed for the 1993 cruise. After subtracting the tidal

Please cite this article in press as: Hernández-Guerra, A., et al. Meridional overturning transports at 7.5N and 24.5N in the Atlantic Ocean during 1992–93 and 2010–11. Prog. Oceanogr. (2014), http://dx.doi.org/10.1016/j.pocean.2014.08.016

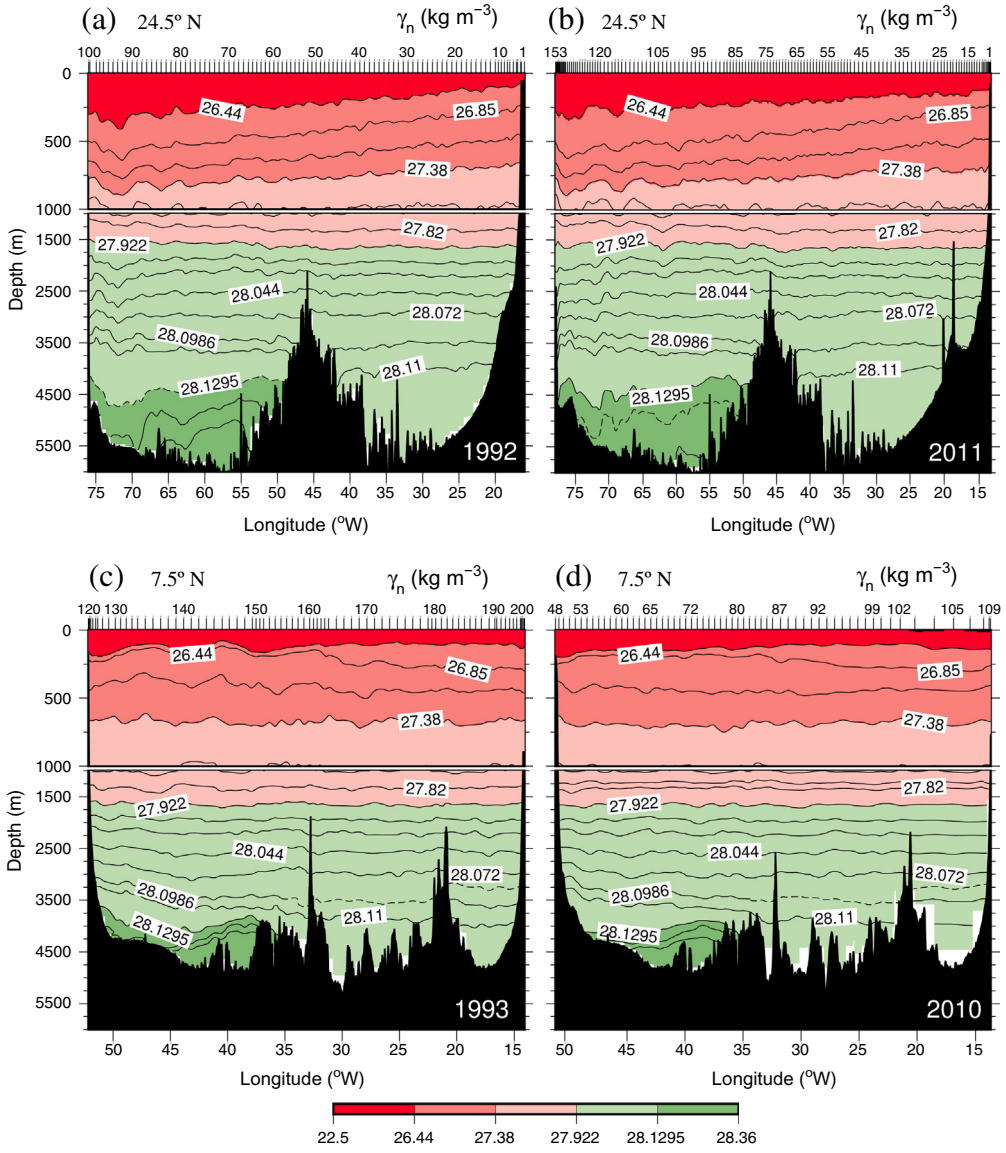

Fig. 5. Vertical sections of neutral density (kg m^{-3}) along 24.5N in (a) 1992 and (b) 2011, and along 7.5N in (c) 1993 and (d) 2010.

velocity, the NBC transport turns out to be 1.3 Sv (through this paper we have used Sv as mass transport, 1 Sv = 10^9 kg/s).

In order to compute the mass and property transports, the water column is divided into a number of γ_n layers, properly specified according to the changing water masses (Table 2). We have selected the same layering as used by Ganachaud (2003a) in global calculations of mass and heat transports using the WOCE zonal sections. Additionally, the Ekman transport at the time of the cruise is calculated using the National Center for Environmental Prediction and National Center for Atmospheric Research (NCEP–NCAR) surface winds; the Ekman transports are then introduced in the first layer for each section (Table 3).

Fig. 6 shows the initial transports through 7.5N and 24.5N and their imbalance (calculated simply as the difference) for each pair of realizations. Adding all layers, the mass transport initially presents a substantially large imbalance, about 16.8 Sv for 1992/93 and 29.6 Sv for 2010/11. In order to reduce them, we set up and apply an inverse box model, which aims at conserving mass. The following equation has to be solved:

$$\iint \rho b\,dx\,dz + A_z(w\bar{\rho}) = -\iint \rho V_r\,dx\,dz + E_k \qquad (1)$$

Table 2
Neutral surface layers, γ_n (kg m^{-3}), and approximate equivalence with water masses: the layers that delimit the water masses are 26.44, 27.38, 27.922, 28.072, and 28.1295 kg m^{-3}, and the sea floor.

Layer	Lower interface (γ_n, kg m^{-3})	Water mass
1	26.44	Surface water
2	26.85	
3	27.162	SACW/NACW
4	27.38	
5	27.62	
6	27.82	AAIW/MW
7	27.922	
8	27.975	
9	28.008	
10	28.044	UNADW
11	28.072	
12	28.0986	
13	28.11	LNADW
14	28.1295	
15	28.141	
16	28.154	AABW
17	Bottom	

Please cite this article in press as: Hernández-Guerra, A., et al. Meridional overturning transports at 7.5N and 24.5N in the Atlantic Ocean during 1992–93 and 2010–11. Prog. Oceanogr. (2014), http://dx.doi.org/10.1016/j.pocean.2014.08.016

Table 3
Ekman transport (Sv) together with its standard deviation for the time of each cruise. Initial value, from NCEP data, and adjusted transport, from the inverse model, are shown.

	1992/1993		2010/2011	
	Initial	Inverse model	Initial	Inverse model
7.5N	9.2 ± 3.2	9.0 ± 2.6	7.2 ± 2.6	7.5 ± 2.7
24.5N	2.8 ± 0.9	2.8 ± 0.8	2.5 ± 1.6	2.5 ± 1.0

where x and z are the along-section and vertical coordinates, respectively; A_z is the horizontal area of each interface; and ρ and $\bar{\rho}$ are the density and the mean density at every interface, respectively. The integral terms are derived from the reference velocity (b) and the relative velocity (V_r), respectively. The second term represents the vertical transfer for each layer, w being an equivalent average dianeutral velocity across the interfaces. The term E_k designates the Ekman transport.

Thus, this model allows us to determine the horizontal velocity at the reference layer (for each station pair) and the mean dianeutral velocity between layers over the region bound by the two transatlantic sections, along with their error covariances (Wunsch, 1996). The specific procedure used with our data set is described in Section 'Model constraints'.

As mass transport is conserved after the inverse model, we estimate the heat transport as:

$$T = \iint \rho C_p \theta v \, dx \, dz \tag{2}$$

where ρ is the density, C_p is the heat capacity of sea water, θ is the potential temperature, and v the absolute cross-section velocity.

The freshwater flux is estimated following Joyce et al. (2001):

$$\tilde{F} = \sum_i \sum_j T_{ij} S'_{ij} / S_0 \tag{3}$$

where T_{ij} is the absolute mass transport in layer i at station pair j, including the Ekman transport in the first layer, S'_{ij} is the anomaly of salinity and S_0 the mean salinity (35.2). Alternatively, we could use some constant S_0; in particular Talley (2008) used a value of 34.9.

Model constraints

The equations for the inverse model consist in total (vertically-integrated) mass conservation and mass conservation per layer, with the possibility of vertical mass exchange between adjacent layers. The Gauss-Markov method is applied to solve the inverse problem (Wunsch, 1996). The solution provided by the method depends on the variance of the velocity field as well as on a set of water transport constraints, with mean values and variances. For the a priori velocity variance, we have assumed either $(0.04\ \mathrm{m\ s^{-1}})^2$ for all stations affected by specific constraints as shown in Table 4 or $(0.02\ \mathrm{m\ s^{-1}})^2$ for the remaining stations.

The a priori variance for each constraint depends on its uncertainty, as well as on a priori uncertainties assigned to each equation. To set these uncertainties for each equation, we have followed the study of Ganachaud (2003b). Accordingly, the uncertainty is largest in the total mass conservation (15.9 Sv), and gradually decreases from the surface layer (8.2 Sv) to the bottom layer (0.5 Sv) to take into account the vertical dependence in baroclinic transport. Additionally, we have also considered mass conservation for 7.5N to be independent of mass conservation for 24.5N, and its uncertainty as given by the flux through the Bering Strait plus its standard deviation (Roach et al., 1995).

We have also included additional constraints for different longitude and depth ranges as described next and shown in Table 4. We have attempted to calculate the Deep Western Boundary Current (DWBC) transport at 7.5N from the 2010 LADCP profiles but failed because of high noise in this westernmost region, near the sea floor. Therefore, the constraint for the DWBC at 7.5N follows the study by Richardson and Schmitz (1993) who found a southward transport of 15 Sv between 900 and 2800 m and a northward recirculation of 6 Sv between 45W and 35W; this pattern of DWBC circulation for 1993 is also observed in the vertical section of oxygen shown by Arhan et al. (1998). We have chosen the uncertainty as half of these transports. The southward DWBC transport across 24.5N was estimated as −26.5 ± 13.5 Sv (Bryden et al., 2005a,b; Johns et al., 2008), not significantly different from recent estimates by Meinen et al. (2013) during 2004–2009.

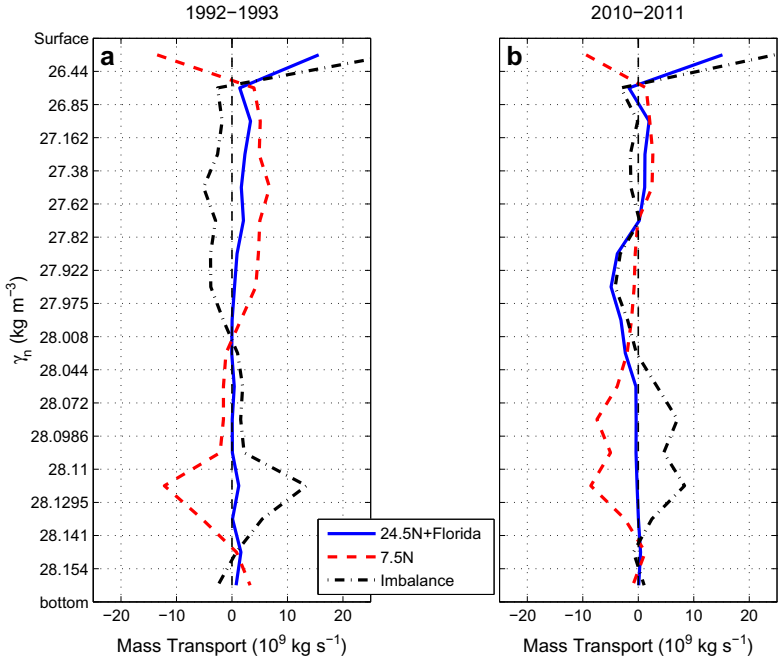

Fig. 6. Initial solution for the zonally integrated mass transports (Sv) per layer across 24.5N and 7.5N, during (a) 1992–1993 and (b) 2010–2011.

Please cite this article in press as: Hernández-Guerra, A., et al. Meridional overturning transports at 7.5N and 24.5N in the Atlantic Ocean during 1992–93 and 2010–11. Prog. Oceanogr. (2014), http://dx.doi.org/10.1016/j.pocean.2014.08.016

Table 4
Specific constraints (Sv) for sections A06 (along 7.5N) and A05 (along 24.5N), for a range of longitudes and layers. Positive transports are to the north. The initial and final transports (respectively calculated as described in the text and as deduced with the inverse model) are shown. DWBC stands for Deep Western Boundary Current, RECIR for the recirculation of DWBC at 7.5N, AABW for Antarctic Bottom Water, and AC for Antilles Current. The eastern end of the Antilles Current was located at about 71.5W during 1992 and near 75.5W in 2011. The Florida Current uses two different constraints, depending on the year: the top value corresponds to 1992 and the bottom one to 2011.

	Long. (W)	Layers	Constraint	1992–3 Initial	1992–3 Final	2010–1 Initial	2010–1 Final
7.5N (A06)							
Bering St.	All	All	−0.8 ± 0.6	11.2	−0.8 ± 3.5	−26.3	−0.8 ± 3.9
DWBC	−52: −45	6: 11	−15 ± 7.5	−17.8	−15.2 ± 2.6	3.6	−11.7 ± 2.7
RECIR	−45: −35	6: 11	6 ± 3	−9.6	3.6 ± 1.3	−9.1	5.0 ± 1.3
AABW	−49: −36	16: 17	1.7 ± 0.6	0.6	1.6 ± 0.9	0.3	1.5 ± 0.8
24.5N (A05)							
Florida Current	Florida Strait	All	31.0 ± 1.0 32.0 ± 2.8	23.0	31.0 ± 0.2	23.0	31.8 ± 0.3
Bering St.	All	All	−0.8 ± 0.6	21.4	−0.8 ± 5.7	−4.1	−0.8 ± 5.4
AC	Diff.	1: 6	6.0 ± 8.1	19.6	18.8 ± 1.6	15.6	12.8 ± 1.0
DWBC	−77: −72	7: 14	−26.5 ± 13.6	16.0	−22.1 ± 4.2	−15.8	−20.1 ± 3.7

Hall et al. (1997) estimated the AABW northward transport at the Equator as 2 ± 4 Sv, as also used by Ganachaud (2003a) in their global inverse model. This value is consistent with our own estimate from LADCP data for 2010 in the western basin, 1.4 ± 0.5 Sv, with the uncertainty estimated after applying a Monte Carlo method to the LADCP velocity error. We use this transport as a constraint for both the 1993 and 2010 cruises across 7.5N.

The Florida Current has been constrained differently for 1992 and 2011. For 1992, the Florida transport has been constrained following the study of Ganachaud (2003a) to be 31 ± 1 Sv. The Florida transport for 2011 was constrained to 32.0 ± 2.8 Sv, estimated with properly calibrated submarine cable voltage data at the time of the cruise (Baringer and Larsen, 2001). Both values are not significantly different.

The Antilles Current and the Deep Western Boundary Current through 24.5N, from the shelf to 72W, have been constrained using in situ mooring data shown in Bryden et al. (2005a,b) and Johns et al. (2008). They found the Antilles Current to flow north from the surface to approximately 1000 m depth, with a transport of 6.0 ± 8.1 Sv. As observed in Fig. 3, the temperature's signal of the Antilles Current in the western margin changes between 1992 and 2011. Its different extension, to about 71.5W in 1992 and to 75.5W in 2011, has been taken into account to constraint the flow.

Final adjusted transport

Layer-integrated transports

The inverse model renders information on the velocity at the reference level, as well as on the mean dianeutral velocities between adjacent layers for the region between 7.5N and 24.5N. Fig. 7 shows the velocity at the reference layer, together with error bars, as a function of longitude. All velocities are small and not significantly different from zero. As in previous inverse solutions, the uncertainties of the reference velocities turn out to be almost equal to the a priori values (Hernández-Guerra et al., 2005; Joyce et al., 2001; Pérez-Hernández et al., 2013).

The mean dianeutral velocities for the region between both transoceanic sections are not significantly different from zero except for the presence of downwelling in the UNADW layers (Fig. 8). In the near-bottom layers, there is weak upwelling from AABW into LNADW, with large uncertainties as in Lumpkin and

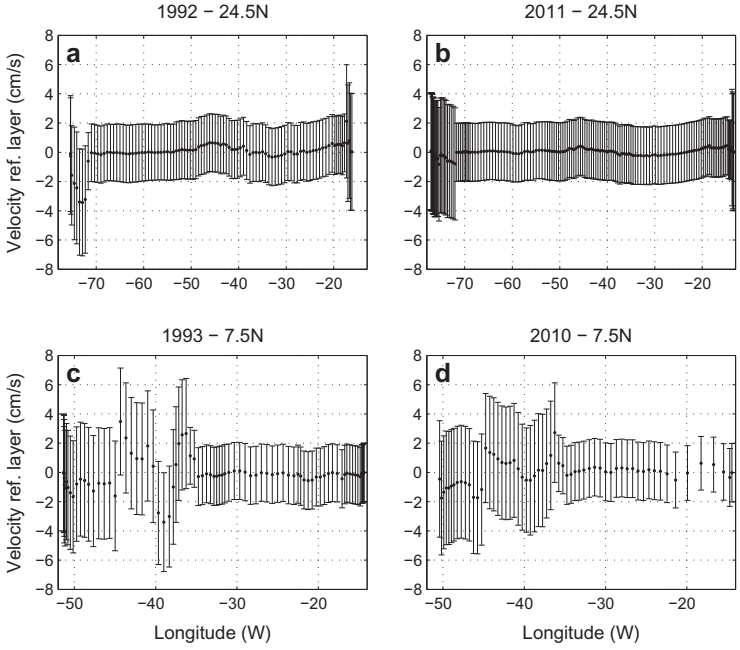

Fig. 7. Reference velocities (cm s^{-1}), with error bars, along 24.5N in (a) 1992 and (b) 2011, and along 7.5N in (c) 1993 and (d) 2010.

Please cite this article in press as: Hernández-Guerra, A., et al. Meridional overturning transports at 7.5N and 24.5N in the Atlantic Ocean during 1992–93 and 2010–11. Prog. Oceanogr. (2014), http://dx.doi.org/10.1016/j.pocean.2014.08.016

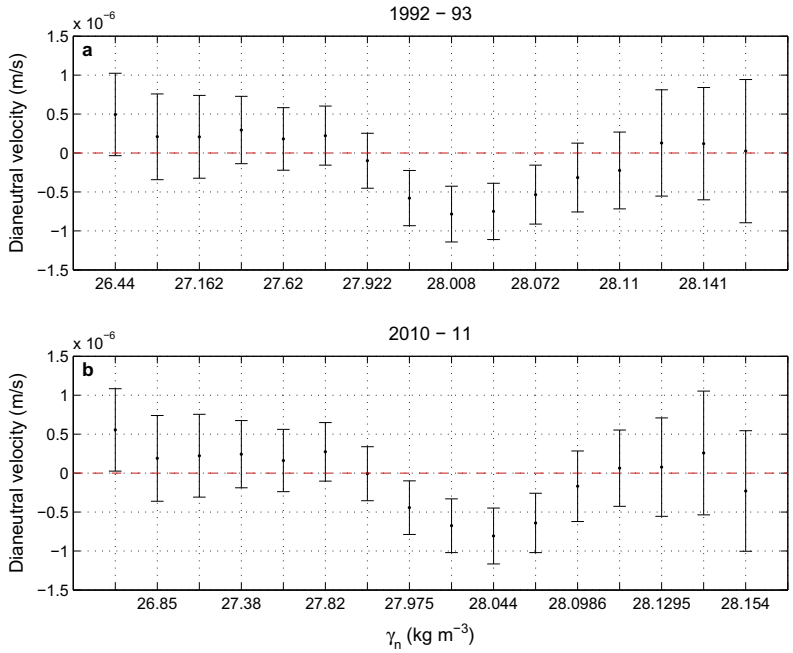

Fig. 8. Dianeutral velocities between layers, corresponding to the mean values over the basin enclosed by the 7.5N and 24.5N sections, with the layers specified as indicated in Table 2.

Speer (2003). The dianeutral velocities calculated for 1992–93 have a similar shape as those estimated by Ganachaud (2003a) using the same data. The main differences are that our downwelling velocities in the UNADW layers are significantly different from zero and our dianeutral velocities in the bottom layers are indistinguishable from zero. The only positive dianeutral velocities, which are significantly different from zero, correspond to the surface-most layer during 2010–11.

The inverse model also provides corrected Ekman transports, although the final estimates are not significantly different from the NCEP/NCAR initial values (Table 3). The adjusted Ekman transport through 7.5N ranges between 9.0 ± 2.6 Sv for 1992 and 7.5 ± 2.7 Sv for 2010, marginally consistent with the value (12.3 ± 1 Sv) provided by Lux et al. (2001) for 1993. The Ekman adjusted transports through 24.5N (2.8 ± 0.8 Sv for 1993 and 2.5 ± 1.0 Sv for 2011) are within the uncertainties of some early estimates (Cunningham et al., 2007) but smaller than others (Lumpkin and Speer (2003) and Atkinson et al. (2012) estimated Ekman transports greater than 4 Sv).

The reference velocities, the dianeutral velocities and the Ekman transport adjusted from the inverse model are used to calculate new mass transports. Fig. 9 shows the zonally integrated

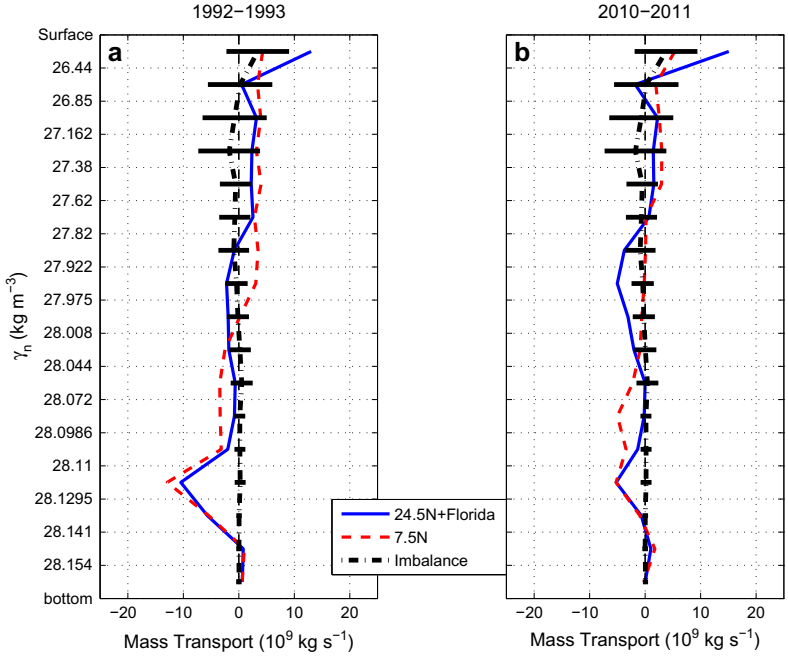

Fig. 9. Zonally integrated mass transport (Sv) per layer across 24.5N and 7.5N, during (a) 1992–1993 and (b) 2010–2011; it is analogous to Fig. 6 but with the reference and dianeutral velocities as estimated from the inverse model. The uncertainties per layer are shown as error bars in the imbalance.

Please cite this article in press as: Hernández-Guerra, A., et al. Meridional overturning transports at 7.5N and 24.5N in the Atlantic Ocean during 1992–93 and 2010–11. Prog. Oceanogr. (2014), http://dx.doi.org/10.1016/j.pocean.2014.08.016

mass transports per layer for the 1992–93 (left plot) and 2010–11 (right plot) surveys. The imbalance per layer is now indistinguishable from zero for both surveys. The total imbalance in mass transport is −0.1 ± 6.0 Sv and 0.0 ± 5.9 Sv for 1992–93 and 2010–11, respectively. Thus, our final circulation patterns are clearly mass conserving. The integrated mass transport per layer for 1993 at 7.5N (Fig. 9a) resembles the transport per layer estimated by Lux et al. (2001) (their Fig. 6) with a different inverse model and using different zonal and meridional sections to close the box.

Table 4 summarizes the constraints for specific layers and longitude ranges together with the calculated initial and adjusted mass transports. The final model transports satisfy all the constraints within one standard deviation of the a priori noise range, except for the relatively large transport of the Antilles Current in 1992. The Antilles Current presents a large temporal variability with transports varying between −15 and +25 Sv (Johns et al., 2008; Lee et al., 1990). Transports within this range may be measured by a single hydrographic section; this is the case with our estimate for section A06 during 1992, the result being consistent with previous estimates (Rintoul and Wunsch, 1991).

The integrated mass transports per layer show a pattern of positive values (transport to the north) in the thermocline and intermediate layers, negative values in the NADW layers, and again positive values in the AABW layers (Fig. 9). The deep southward flow at 24.5N presents two lobes, an upper lobe, corresponding to the UNADW formed in the Labrador Sea, and a deeper lobe, corresponding to the LNADW of overflow waters. At 7.5N, only the deeper lobe is recognizable, spanning a water column thicker than at 24.5N.

The gross vertical patterns for the 1992–93 and 2010–11 integrated mass transports are qualitatively similar though they differ in some details (Fig. 9). The main differences are (1) that northward transport in the deep central water and intermediate water layers is greater in 1992–93 than in 2010–11, and (2) the southward transport of the upper/lower lobe of deep waters is smaller/larger in 1992–93 than in 2010–11.

The meridional transports through 7.5N and 24.5N, as deduced from the inverse model, are integrated for different strata, westwards from the African coast (Figs. 10 and 11). Each stratum incorporates several adjacent layers having the net transport with one same direction, as shown in Table 5. At 7.5N, there is northward transport in the thermocline and intermediate strata (layers 1:9 for 1993 and layers 1:7 for 2010), a southward transport in the deep stratum (layers 10:15 for 1993 and layers 8:15 for 2010), and a

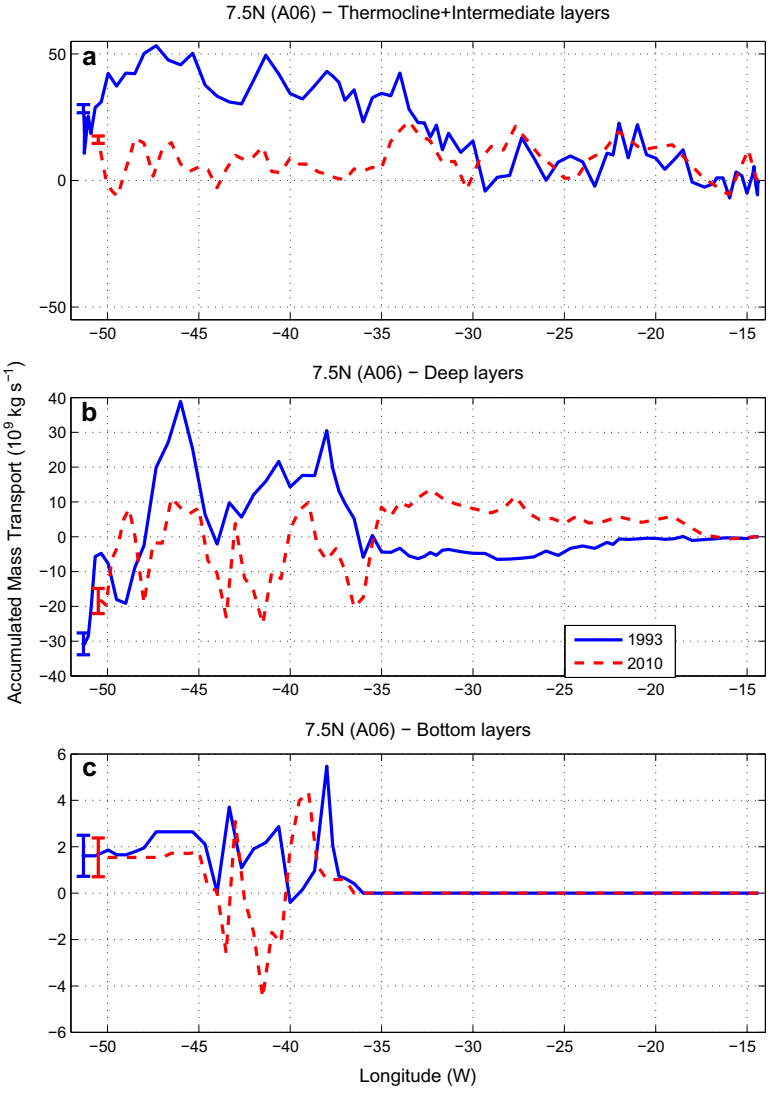

Fig. 10. Westward accumulated mass transport at 7.5N (section A06) for (a) surface and intermediate, (b) deep, and (c) bottom layers for 1993 (solid lines) and 2010 (dashed lines).

Please cite this article in press as: Hernández-Guerra, A., et al. Meridional overturning transports at 7.5N and 24.5N in the Atlantic Ocean during 1992–93 and 2010–11. Prog. Oceanogr. (2014), http://dx.doi.org/10.1016/j.pocean.2014.08.016

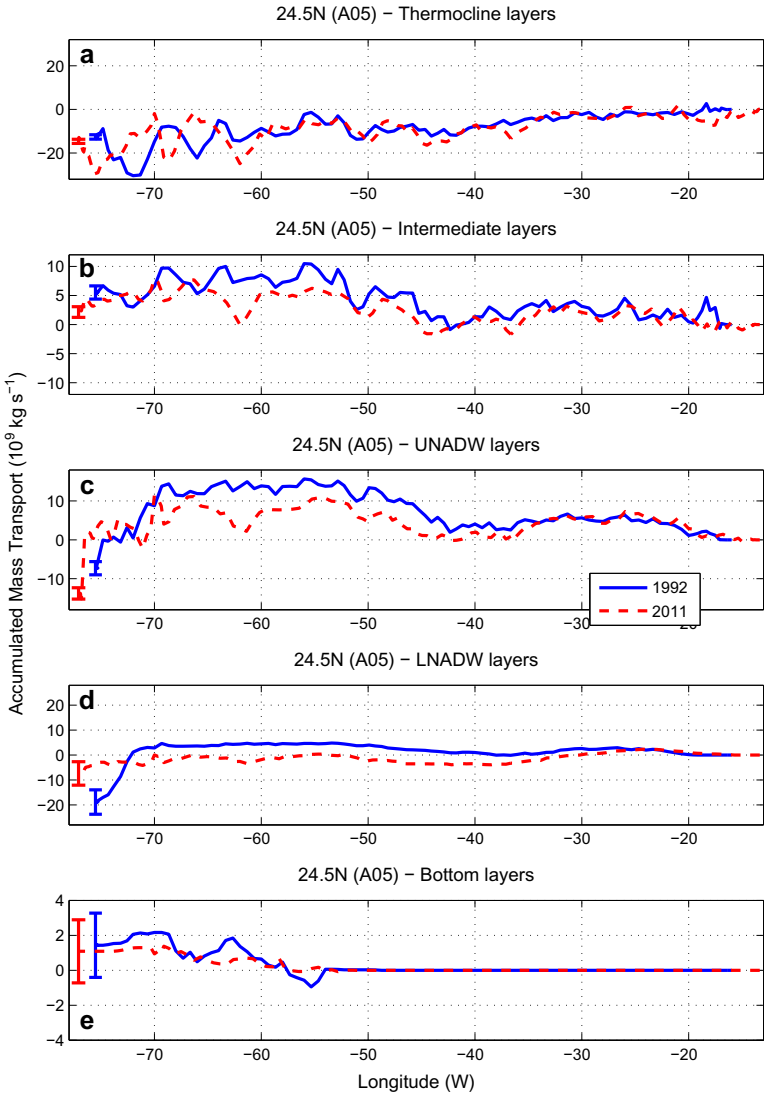

Fig. 11. Westward accumulated mass transport at 24.5N (section A05) for (a) surface, (b) intermediate, (c) UNADW, (d) LNADW, and (e) bottom layers for 1992 (solid lines) and 2011 (dashed lines).

Table 5
Accumulated mass transports (Sv) for different layers. Transport is summed over consecutive layers with the same flow direction; value through section A05 (along 24.5N) is divided into UNADW and LNADW. The Ekman transport has been included in the thermocline layer.

	7.5N (A06)		24.5N (A05)		24.5N + Florida (A05)	
	1993	2010	1992	2011	1992	2011
Thermocline			−12.6 ± 1.0	−14.6 ± 1.0	16.7 ± 1.0	17.0 ± 0.9
Intermediate	28.4 ± 1.6	16.1 ± 1.5	5.5 ± 1.1	2.1 ± 0.9	7.1 ± 1.1	2.2 ± 0.9
Deep						
UNADW	−30.8 ± 3.1	−18.4 ± 3.6	−7.3 ± 1.7	−13.8 ± 1.5	−26.2 ± 5.2	−21.2 ± 4.9
LNADW			−18.8 ± 4.9	−7.4 ± 4.7		
Bottom	1.6 ± 0.9	1.5 ± 0.8	1.4 ± 1.8	1.1 ± 1.8	1.4 ± 1.8	1.1 ± 1.8

northward transport in the bottom stratum. At 24.5N, excluding the Florida Strait transport, there is a southward transport in the thermocline stratum (layers 1:3 for 1992 and layers 1:4 for 2011) and a northward transport in the intermediate layers (layers 4:6 for 1992 and layers 5:6 for 2011); the deep stratum (layers 7:15) flows south composed by both UNADW (layers 7:11) and LNADW (layers 12:15) and the AABW stratum moves northwards.

At 7.5N, the integrated northward joint mass transport for the thermocline and intermediate strata is significantly different during both realizations, 28.4 ± 1.6 Sv during 1993 and 16.1 ± 1.5 Sv during 2010 (Table 5). The main reason for this difference probably comes from the time of the cruise and the seasonality of the North Equatorial Counter Current (NECC) (Katz and Garzoli, 1982; Stramma and Schott, 1999); during the months of the 2010 cruise (April and May) a well-developed NECC diverted waters towards the east while at the time of the 1993 cruise (February and March) the NECC had not yet developed and the NBC followed swiftly into the Caribbean Sea. At 24.5N, the transport in the

Please cite this article in press as: Hernández-Guerra, A., et al. Meridional overturning transports at 7.5N and 24.5N in the Atlantic Ocean during 1992–93 and 2010–11. Prog. Oceanogr. (2014), http://dx.doi.org/10.1016/j.pocean.2014.08.016

thermocline stratum was not significantly different in 1992 (16.7 ± 1.0 Sv) and 2011 (17.0 ± 0.9 Sv). The intermediate water transports were substantially different, 5.5 ± 1.1 Sv in 1992 in comparison to 2.1 ± 0.9 Sv in 2011, reflecting a significant decrease in transport.

At 7.5N, the southward transport of NADW shows a significant decrease between both realizations, from −30.8 ± 3.1 Sv in 1993 to −18.4 ± 3.6 Sv in 2010 (Fig. 10b). In contrast, at 24.5N the total transport of NADW to the south is not significantly different during both realizations, with −26.2 ± 5.2 Sv in 1992 and −21.2 ± 4.9 Sv in 2011 (Table 5). Transports at 24.5N are consistent with previous estimates, in the range from −15 to −25 Sv, as obtained from different inverse models (Lumpkin and Speer, 2003; Macdonald, 1998; Roemmich and Wunsch, 1985; Wunsch and Grant, 1982). Although the total NADW transport does not change, its distribution between UNADW and LNADW does: an increase of southward transport of UNADW at 24.5N, from −7.3 ± 1.7 Sv in 1992 to −13.8 ± 1.5 Sv in 2011, is compensated with a decrease of southward transport of LNADW, from −18.8 ± 4.9 Sv in 1992 to −7.4 ± 4.7 Sv in 2011 (Table 5 and Fig. 11c and d). This compensation was also observed by Cunningham et al. (2007) with the Rapid-WATCH data and by Atkinson et al. (2012) with the transoceanic sections carried out at 24.5N.

The northward transport of AABW, which takes place west of the MAR, shows a (non-significant) decrease as we move between 7.5N and 24.5N: from 1.6 ± 0.9 Sv to 1.4 ± 1.8 in 1992/93, and from 1.5 ± 0.8 Sv to 1.1 ± 1.8 Sv in 2010/11. This progressive decreases to the north is to be expected because of the southern origin of these waters, and has also been reported by Ganachaud (2003a). Nevertheless, because of the uncertainty of these transports, we cannot confirm the decreasing trend between 1981 and 2004 proposed by Johnson et al. (2008). Frajka-Williams et al. (2011) used reference levels of 3200/4100 db to estimate the transport of AABW in 1992 as 2.5/3.1 Sv, which lie in the range of our results.

We may compare the water mass transports for different strata during February 2011, as calculated with the inverse model applied to the A05 section along 24.5N and as deduced from the Rapid-WATCH array at 26.5N (Fig. 12). The Rapid-WATCH array is a unique system which, since 2004, provides a continuous time series of mass transport at 26.5N (Johns et al., 2011). Water transport is estimated from a combination of Ekman transport inferred from satellite data, transport by the Florida Current as deduced from cable voltage measurements, transport in the western boundary region as inferred from moored current-meters, and geostrophic transport estimates in the ocean interior from moored temperature and salinity sensors installed in both ocean margins and in the MAR. The Rapid-WATCH system balances mass by imposing a constant velocity value to the whole transoceanic section.

The comparison is not straight-forward as Rapid-WATCH divides the water column in pressure levels (0–800 m, thermocline; 800–1100 m, intermediate; 1100–3000 m, UNADW; 3000–5000 m, LANDW; and AABW, from 5000 m down to the sea floor) rather than neutral density levels as we do. For the comparison, we have chosen those density layers that best represent the different Rapid-WATCH depth strata: 27.38, 27.922, 28.072, and 28.1295 kg m^{-3}, and the sea bottom (Table 2). Fig. 5 clearly shows that this is a rough approximation, particularly for the thermocline waters (the 27.38 kg m^{-3} isoneutral slopes between about 850 m in the western margin to 700 m in the eastern margin) and the intermediate waters (the 27.922 kg m^{-3} isoneutral is close to 1500 m throughout the section). Despite these limitations, the comparison shows fairly good agreement between the two sets of values, with values which are not significantly different for the UNADW, LNADW and AABW strata.

Circulation patterns

The model allows computing the distribution of the meridional velocities along all transoceanic sections (Fig. 13). In all sections we may appreciate the existence of substantial variability, as characterized by the changing sign of the latitudinal velocity, with the largest reversals in the western basin. The intermittency occurs at scales of several degrees, pointing at a mesoscalar origin; nevertheless, some of the currents remain intense (greater than 0.10 m s^{-1}) down to 500 m or more, suggesting they respond to meandering associated to or eddies detaching from large-scale currents. The intermittency is greatest at 7.5N during the 1993 realization; since this section was carried out at a time of the year (winter) when the NBC did not retroflect, it seems probable that some of this variability originated at the boundary current. The boundary current systems are remarkably clear at 7.5N, with very intense currents at both central and deep water levels in the western boundary and

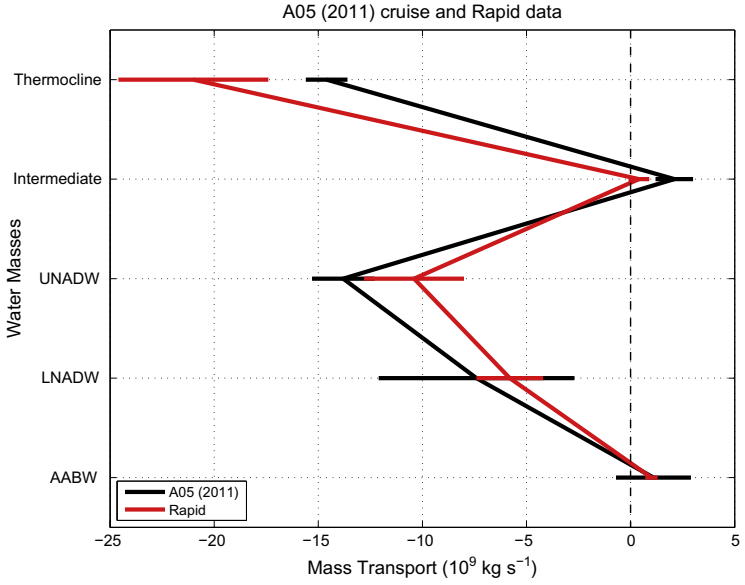

Fig. 12. Mass transport per stratum, as calculated by the inverse model (black line) for section A05 carried out in 2011 along 24.5N, and by the Rapid-WATCH array (gray line) along 26.5N during the time of the cruise. See Table 2 for the definition of the different strata.

Please cite this article in press as: Hernández-Guerra, A., et al. Meridional overturning transports at 7.5N and 24.5N in the Atlantic Ocean during 1992–93 and 2010–11. Prog. Oceanogr. (2014), http://dx.doi.org/10.1016/j.pocean.2014.08.016

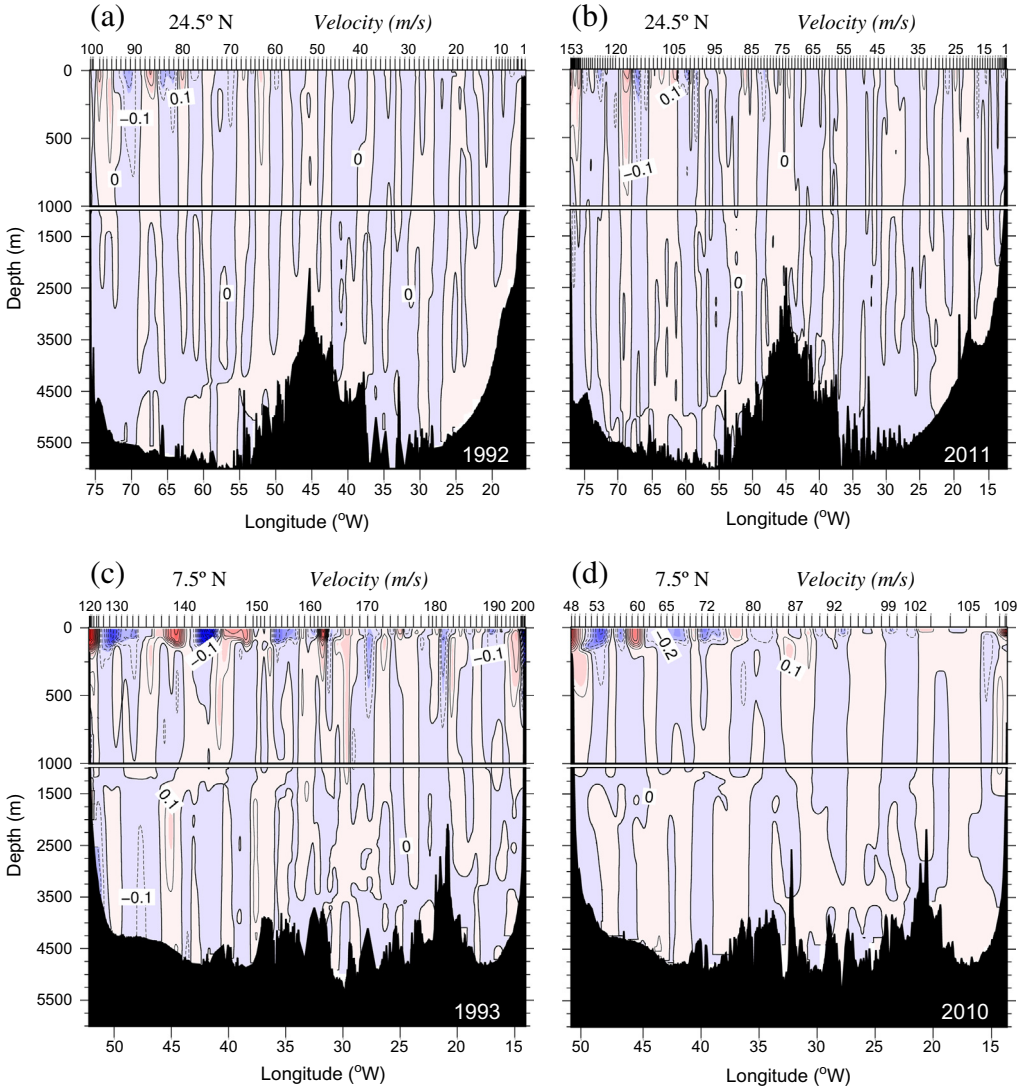

Fig. 13. Vertical sections of latitudinal velocity (m s^{-1}) along 24.5N in (a) 1992 and (b) 2011, and along 7.5N in (c) 1993 and (d) 2010. Notice the change in the vertical scale, with an expanded view of the top 1000 m of the water column. Contours are drawn every 0.1 m s^{-1}, with solid/dashed contours representing positive/negative values (northward/southward velocities).

fairly intense currents at central levels in the eastern boundary. At 24.5N the western boundary current displays the existence of the Antilles Current; recall most of the northward transport occurs in the Florida Straits, which are not included.

The NBC shows up clearly in the western boundary during both 7.5N realizations (Figs. 10c and d and 13). The NBC in 1993 is located about 1° closer to shore (50.9W) as compared with 2010 (49.6W). A previous estimate of the mean NBC transport was 16 ± 2 Sv, but with high variability, reaching maximum values of 31.8 ± 2 Sv (Garzoli et al., 2004; Johns et al., 1998; Zhang et al., 2011). In particular, using the same 1993 data set, Lux et al. (2001) estimated the NBC transport to be 17.9 ± 2 Sv. Our estimate for the NBC depends on how we define its offshore limit but the westward accumulated mass transports (Table 5) are consistent with these numbers.

The 24.5N realizations may be used to obtain estimates for the Canary and Antilles Currents. The transport between the eastern boundary and 20W is −2.1 ± 0.9 Sv for 1992 and −2.3 ± 1.1 Sv for 2011, consistent with previous Canary Current estimates (Machín et al., 2006). The change in transport in the western boundary, from the minimum accumulated transport west of 70W to the western end, gives an estimate for the Antilles Current in the thermocline layer: 17.7 ± 1.4 Sv in 1992 and 14.8 ± 0.7 Sv in 2011. Ganachaud (2003a) estimated the Antilles Current to be 27 ± 3 Sv, larger than ours presumably because their global model did not constrain the transport of the boundary current.

At 7.5N, the DWBC is estimated to transport −26.0 ± 1.3 Sv to the south in 1993, only partly compensated with a northward recirculation of 14.4 ± 2.2 Sv (Fig. 10b); this value is less than estimated by Lux et al. (2001) using the same data. In 2010, however, the northward recirculation current approximately balances the transport of the DWBC. At 24.5N, the DWBC, defined here as the transport west of 70W in deep layers, shows not significantly different transports in 1992 (−37.8 ± 5.4 Sv) and 2011 (−28.8 ± 6.3 Sv) (Fig. 11c and d). Toole et al. (2011), using data from an array of current meters located at about 39N, 70W (the so-called line W), estimated a mean DWBC transport of −25.1 ± 12.5 Sv. Although a comparison of the transport estimate through line W and the meridional transport at 24.5N is not straightforward, because of possible recirculations and entrainment of water masses along the path of the DWBC between both latitudes, the consistency of our results with those from Toole et al. (2011) is encouraging.

Please cite this article in press as: Hernández-Guerra, A., et al. Meridional overturning transports at 7.5N and 24.5N in the Atlantic Ocean during 1992–93 and 2010–11. Prog. Oceanogr. (2014), http://dx.doi.org/10.1016/j.pocean.2014.08.016

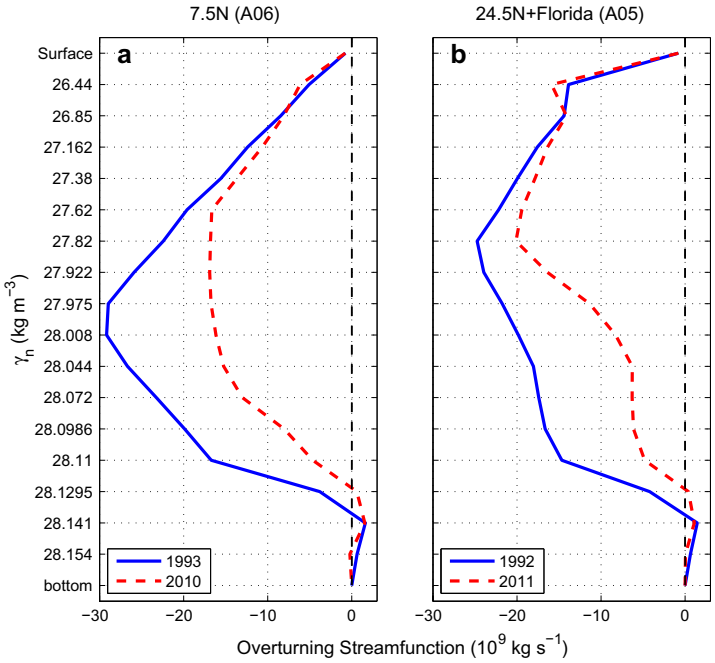

Fig. 14. Overturning stream function across sections (a) 7.5N and (b) 24.5N. This function corresponds to the mass transport integrated from the bottom.

Table 6
AMOC transports (Sv) through sections A06 (along 7.5N) and A05 (along 24.5N).

	7.5N (time of the year)	24.5N (time of the year)
1992–93	29.2 ± 1.7 (February–March)	24.7 ± 1.7 (July–August)
2010–11	16.9 ± 1.5 (April–May)	20.1 ± 1.4 (January–March)

Atlantic Meridional Overturning Circulation, heat and freshwater flux

We may calculate the intensity of the overturning as the maximum mass transport, calculated through depth integration from the sea surface, typically comprising thermocline and intermediate waters. We may compute the meridional overturning function by simply adding the layer transports from either the bottom or the sea surface. Fig. 14 illustrates this summation for both latitudes, calculated with the summation starting at the sea floor. The AMOC turns out to be weaker in 2010–11 than in 1992–93 for both latitudes (Table 6), the difference being substantially larger at 7.5N (16.9 ± 1.5 Sv versus 29.2 ± 1.7 Sv) than at 24.5N (20.1 ± 1.4 Sv versus 24.7 ± 1.7 Sv).

Our AMOC estimate at 24.5N in 1992 (24.7 ± 1.7 Sv) is larger than values obtained in previous studies, yet it is consistent with the mean value and high variability found at 26.5N with one year of continuous measurements through the Rapid-WATCH mooring array, 18.7 ± 5.6 Sv (Cunningham et al., 2007). This variability has been recently confirmed by the analysis of the extended Rapid-WATCH data set (Johns et al., 2011; Smeed et al., 2014). Our estimate for 7.5N in 1993 (29.2 ± 1.7 Sv) is also greater than the value estimated by Lux et al. (2001) (22 Sv) although these authors do not provide uncertainty values.

The heat flux through 7.5N is estimated as 0.7 ± 0.1 PW in 1993 and 0.6 ± 0.1 PW in 2010. Previous studies (Ganachaud and Wunsch, 2003; Talley, 2003; Macdonald, 1998; Friedrichs and Hall, 1993) give very diverse results, ranging between 0.3 and 1.39 PW. A limitation in all these studies is the lack of reliable velocity data over the American continental platform, where the NBC may transport a substantial amount of water and heat. Ganachaud and Wunsch (2003) added a water transport of 5 Sv with a temperature of 26 °C, increasing its estimate from 1.0 ± 0.55 PW to 1.26 ± 0.31 PW. If we included a transport of 5 Sv instead of our SADCP-based estimate of 1.3 Sv, the heat transport would increase to 1.2 PW in 1993 and 1.1 PW in 2010, similar to Ganachaud and Wunsch (2003).

At 24.5N, we estimate the heat flux to be 1.4 ± 0.1 PW in 1992 and 1.2 ± 0.1 PW in 2011. Despite the substantial decrease from 1992 to 2011 in the intensity of the AMOC (4.6 Sv, Table 6), the heat flux is similar for both years; this is slightly less than the expected change in heat transport (0.3 PW), according to Johns et al.'s (2011) heat-to-mass transport ratio (a change in 0.064 PW for each Sv). The reason lies in the source of the transport changes, not in the thermocline but rather on intermediate waters (Table 5), which hold less heat than the surface layers. The heat flux at 24.5N has been previously calculated on several occasions, with different methodologies, all leading to reasonably consistent values. Macdonald (1998), Hall and Bryden (1982), Talley (2003), Ganachaud and Wunsch (2003), and Lavín et al. (2003) estimated the heat transport to be 1.07, 1.2, 1.28, 1.27 ± 0.15, and 1.51 ± 0.39 PW, respectively.

For our two-section closed box, the net loss of freshwater has significantly decreased from 1992–93 (−0.47 ± 0.05 Sv) to 2010–11 (−0.36 ± 0.03 Sv). Accordingly, in the area enclosed by the zonal sections at 7.5N and 24.5N the excess evaporation over precipitation has decreased or, equivalently, the salinity flux into the region has been reduced; in particular, we note that these results are insensitive, to the second decimal digit, to our selection of 34.9 or 35.2 for S_0.

Discussion and conclusions

We have applied the same inverse model to the transatlantic sections carried out at 7.5N and 24.5N in 1992–93 and 2010–11. Thus, any differences in the ocean circulation patterns, as well as in the transport of mass, heat and freshwater, must reflect actual changes in the hydrographic data. In particular, the analysis has allowed us to explore how the AMOC evolves between tropical and subtropical waters of the North Atlantic Ocean and how its intensity changes between 1992–93 and 2010–11.

Please cite this article in press as: Hernández-Guerra, A., et al. Meridional overturning transports at 7.5N and 24.5N in the Atlantic Ocean during 1992–93 and 2010–11. Prog. Oceanogr. (2014), http://dx.doi.org/10.1016/j.pocean.2014.08.016

The transports through the 24.5N section, the transoceanic section with the largest number of realizations (six times), have been presented in several papers using different methodologies. A recent analysis of the first five cruises was conducted by Atkinson et al. (2012). Their results for the 1992 cruise, without uncertainty values, display some similarities but also some disagreements with our own calculations. Their upper thermocline mass transport (17.7 Sv) is not significantly different from our calculated transport (16.7 ± 1.0 Sv). They also find an increase/decrease of the fractions of UNADW/LNADW transport from 1992 to 2010, and the AABW transport remains almost unchanged. The main difference is the mass transport at intermediate layers. They find a transport of only 0.7 Sv in 1992, well in the middle of the range of transports found for the five realizations (from −0.3 Sv in 1998 to 1.6 Sv in 1957). In contrast, we find substantially larger transports, 5.5 ± 1.1 Sv in 1992 and 2.1 ± 0.9 Sv in 2011.

A remarkable result is the substantial change in the spatial structure of the transport per water strata, as well as in the intensity of the AMOC, at 7.5N. During 1993 the major northward transport of thermocline and intermediate waters occurred near the MAR and the NBC had a relatively weak contribution; during 2010, instead, there was no net northward contribution near the MAR and most of the net transport took place near the western boundary. During 1993 the deep layers displayed some northward transport in the western basin while in 2010 it occurred in the eastern basin; in both occasions, however, the net flow was towards the south as a result of the Deep Western Boundary Current.

Some of this variability may be related to seasonal changes in both the formation of deep waters and in the western boundary current system. Deep water formation in the subpolar North Atlantic takes place at times of maximum surface cooling, about January and February. The Deep Western Boundary Current will take several months to reach from the formation region to the subtropics; Kanzow et al. (2010) have indeed showed that, at the RAPID-Watch array, the AMOC is weaker in February–March (at the time of the 2011 section) than in July–August (when the 1992 section was done). Additionally, the returning limb of the AMOC depends on the seasonality in the intensity of the NBC and its retroflection. The NBC has minimum values in April–May and maximum ones in July–August (Johns et al., 1998), but the inter-hemispheric transport depends largely on the intensity of the retroflection either as the Equatorial Undercurrent (Brandt et al., 2006) or the NECC (Schouten et al., 2005), which reach maximum values in summer and early fall.

The zonal patterns of mass transport (Fig. 10) strongly suggest some coupling between the returning limb (thermocline and intermediate strata) and the formation limb (deep waters) which is consistent with long term changes. San Antolín Plaza et al. (2012) examined the changes in the structure of the water mass along 7.5N using the 1957 (IGY), 1993 (WOCE) and 2010 cruises, and concluded that during the whole time period there has been an increase in the presence of (increasingly warmer and saltier) deep waters at the expense of intermediate waters. The reduction in intermediate waters is consistent with our observation of a significant decrease in central and intermediate water transports (Fig. 10 and Table 5); yet the increased presence of NADW is accompanied by a substantial decrease, almost halving, in the transport of deep waters (Table 5). The explanation may be related to the proximity of the formation regions: the closer the formation region the greater will be the influence of this water mass even at times of weak transport.

Both sets of realizations (1992/93 and 2010/11) share two important properties. The first one is the presence of the starting and returning limbs of the AMOC respectively comprising the central-intermediate and deep strata (Fig. 14). The second one is the existence of two cores of southward flow at 24.5N, located in the lower part of the LNADW and the whole UNADW strata (Fig. 14b), in contrast with one single core of southward flow at 7.5N which occupies the whole LNADW and the bottom portion of the UNADW strata (Fig. 14a). Between both sections there is a redistribution of the fractions of southward flowing waters from the UNADW towards the LNADW (Fig. 8).

Finally, our calculations of heat transport at 24.5N for 1992 (1.4 ± 0.1 PW) and 2011 (1.2 ± 0.1 PW) fit well in the range of previous estimates. In particular, the 2011 value is similar to the value estimated by Johns et al. (2011), 1.33 ± 0.40 PW, obtained using 3.5 years of Rapid-WATCH measurements. Similarly, the heat transport at 7.5N did not change much between 1993 and 2010, decreasing from 0.7 ± 0.1 PW to 0.6 ± 0.1 PW. The reduction in heat transport at 24.5N is similar to the reduction in water transport (19% and 14%, respectively) but the reduction in heat transport at 7.5N is substantially smaller than the reduction in water transport (19% as compared to 42%). This is because the heat transport through 7.5N strongly depends on the mass transport along the Brazil continental shelf, which we have selected to be the same for both realizations.

It is probably adequate to finish with a few caution words on interpreting the above results in terms of long-term changes in the intensity of the AMOC. The first warning comes, as discussed above, from the comparison of sections sampled at different seasons. This is critical for the thermocline and intermediate layers because of the very intense seasonality in the equatorial and tropical current system, affecting not only the western boundary current but also the interior flows as a result of the seasonal displacement of the Inter-Tropical Convergence Zone. It is also likely important for the deep layers, particularly as we get closer to the deep water formation regions. The second caution relates to the common assumption that the circulation pattern, that comes out from the analysis of sections carried out during the same or nearby years, can be taken as instantaneous shots of the vertical structure of the MOC. This is not necessarily true as the thermocline and deep ocean circulation may take quite different times to travel between sections that are separated by several hundred or thousand kilometers. For example, a water parcel moving 0.05 m s^{-1} would take 1.2 years to travel the distance between 7.5N and 24.5N, or 6 years if moving at 0.01 m s^{-1}, velocities typical of the deep layers; however, a water parcel near the surface that moves at 0.5 m s^{-1} would take only 44 days. This simple consideration, in the middle of a plethora of seasonal, inter-annual and inter-decadal variations, points at non-trivial ways of interaction between the upper and deep oceans.

Acknowledgements

This work has been performed under the projects MOC2 (CTM2008-06438) and Malaspina (CSD2008-00077), funded by the Spanish Government and Feder. Part of this study was carried out when the first author spent a sabbatical at Scripps Institution of Oceanography with a grant from "el Programa Nacional de Movilidad de Recursos Humanos del Plan Nacional de I+D+I". The authors thank the captain and the crew of the R/V Sarmiento de Gamboa and the R/V Hespérides as well as the Unidad Tecnológica Marina (UTM) for their help at sea. Special thanks go to David Sosa Trejo for helping with data treatment and Figs. We are grateful to Eleanor Frajka-Williams and two anonymous Reviewers for a number of constructive comments and suggestions.

References

Arhan, M., Colin de Verdière, A., Mémery, L., 1994. The eastern boundary of the subtropical North Atlantic. Journal of Physical Oceanography 24, 1295–1316.

Arhan, M., Mercier, H., Bourles, B., Gouriou, Y., 1998. Hydrographic sections across the Atlantic at 7:30N and 4:30S. Deep Sea Research Part I 45, 829–872.

Atkinson, C.P., Bryden, H.L., Cunningham, S.A., King, B.A., 2012. Atlantic transport variability at 25°N in six hydrographic sections. Ocean Science 8, 497–523.
Baringer, M.O., Larsen, J., 2001. Sixteen years of Florida current transport at 27°N. Geophysical Research Letters 28, 3179–3182.
Baringer, M., Molinari, R., 1999. Atlantic Ocean baroclinic heat flux at 24 to 26N. Geophysical Research Letters 26, 353–356.
Bourles, B., Molinari, R.L., Johns, E., Wilson, W.D., Leaman, K.D., 1999. Upper layer currents in the western tropical North Atlantic (1989–1991). Journal of Geophysical Research 104, 1361–1375.
Brandt, Peter, Schott, Friedrich A., Provost, Christine, Kartavtseff, Annie, Hormann, Verena, Bourlès, Bernard, Fischer, Jürgen, 2006. Circulation in the central equatorial Atlantic: mean and intraseasonal to seasonal variability. Geophysical Research Letters 33. http://dx.doi.org/10.1029/2005GL025498.
Bryden, H., Johns, W., Saunders, P., 2005a. Deep western boundary current east of Abaco: mean structure and transport. Journal of Marine Research 63, 35–57.
Bryden, H.L., Longworth, H.R., Cunningham, S.A., 2005b. Slowing of the Atlantic meridional overturning circulation at 25°N. Nature 438, 655–657.
Cunningham, S.A., Kanzow, T., Rayner, D., Baringer, M.O., Johns, W.E., Marotzke, J., Longworth, H.R., Grant, E.M., Hirschi, J.J.M., Beal, L.M., Meinen, C.S., Bryden, H.L., 2007. Temporal variability of the Atlantic meridional overturning circulation at 26.5N. Science 317, 935–938.
Dickson, R.R., Brown, J., 1994. The production of North Atlantic Deep Water: sources, rates, and pathways. Journal of Geophysical Research 99, 12319–12341.
Fraile-Nuez, E., Hernández-Guerra, A., 2006. Wind-driven circulation for the eastern North Atlantic Subtropical Gyre from Argo data. Geophysical Research Letters 33, L03601. http://dx.doi.org/10.1029/2005GL025122.
Fraile-Nuez, E., Machín, F., Vélez-Belchí, P., López-Laatzen, F., Borges, R., Benítez-Barrios, V., Hernández-Guerra, A., 2010. Nine years of mass transport data in the eastern boundary of the North Atlantic Subtropical Gyre. Journal of Geophysical Research – Oceans 115, C09009. http://dx.doi.org/10.1029/2010JC006161.
Frajka-Williams, E., Cunningham, S.A., Bryden, H., King, B.A., 2011. Variability of Antarctic Bottom Water at 24.5°N in the Atlantic. Journal of Geophysical Research 116, C11026. http://dx.doi.org/10.1029/2011JC007168.
Friedrichs, M.A., Hall, M.M., 1993. Deep circulation in the tropical North Atlantic. Journal of Marine Research 51, 697–736.
Fuglister, F.C., 1960. Atlantic Ocean Atlas of Temperature and Salinity Profiles and Data from the International Geophysical Year of 1957–1958. The Woods Hole Oceanographic Institution Atlas Series.
Ganachaud, A., 2003a. Large-scale mass transports, water mass formation, and diffusivities estimated from World Ocean Circulation Experiment (WOCE) hydrographic data. Journal of Geophysical Research 108 (C7), 3213. http://dx.doi.org/10.1029/2002JC001565.
Ganachaud, A., 2003b. Error budget of inverse box models: the North Atlantic. Journal of Atmospheric and Oceanic Technology 20, 1641–1655.
Ganachaud, A., Wunsch, C., 2000. Improved estimates of global ocean circulation, heat transport and mixing from hydrographic data. Nature 408, 453–457.
Ganachaud, A., Wunsch, C., 2003. Large-scale ocean heat and freshwater transports during the World Ocean Circulation Experiment. Journal of Climate 16, 696–705.
Garzoli, S.L., Ffield, A., Johns, W.E., Yao, Q., 2004. North Brazil Current retroflection and transports. Journal of Geophysical Research: Oceans 109, C01013. http://dx.doi.org/10.1029/2003JC001775.
Hall, M., Bryden, H., 1982. Direct estimates and mechanisms of ocean heat-transport. Deep-Sea Research 29, 339–359.
Hall, M., McCartney, M., Whitehead, J., 1997. Antarctic Bottom Water flux in the equatorial western Atlantic. Journal of Physical Oceanography 27, 1903–1926.
Harvey, J., 1982. θ–S relationships and water masses in the eastern North Atlantic. Deep-Sea Research 29, 1021–1033.
Hernández-Guerra, A., Nykjaer, L., 1997. Sea surface temperature variability off north-west Africa: 1981–1989. International Journal of Remote Sensing 18, 2539–2558.
Hernández-Guerra, A., Fraile-Nuez, E., Borges, R., López-Laatzen, F., Vélez-Belchí, P., Parrilla, G., Muller, T., 2003. Transport variability in the Lanzarote passage (eastern boundary current of the North Atlantic subtropical Gyre). Deep Sea Research Part I 50, 189–200.
Hernández-Guerra, A., Fraile-Nuez, E., López-Laatzen, F., Martínez, A., Parrilla, G., Vélez-Belchí, P., 2005. Canary Current and North Equatorial Current from an inverse box model. Journal of Geophysical Research 110, C12019. http://dx.doi.org/10.1029/2005JC003032.
Hernández-Guerra, A., Joyce, T.M., Fraile-Nuez, E., Vélez-Belchí, P., 2010. Using Argo data to investigate the meridional overturning circulation in the North Atlantic. Deep Sea Research Part I 57, 29–36.
Iorga, M.C., Lozier, M.S., 1999. Signatures of the Mediterranean outflow from a North Atlantic climatology 2. Diagnostic velocity fields. Journal of Geophysical Research 104, 26011–26026.
Johns, W., Lee, T., Beardsley, R., Candela, J., Limeburner, R., Castro, B., 1998. Annual cycle and variability of the North Brazil Current. Journal of Physical Oceanography 28, 103–128.
Johns, W.E., Beal, L.M., Baringer, M.O., Molina, J.R., Cunningham, S.A., Kanzow, T., Rayner, D., 2008. Variability of shallow and deep western boundary currents off the Bahamas during 2004–05: results from the 26°N RAPID-MOC array. Journal of Physical Oceanography 38, 605–623.
Johns, W.E., Baringer, M.O., Beal, L.M., Cunningham, S.A., Kanzow, T., Bryden, H.L., Hirschi, J.J.M., Marotzke, J., Meinen, C.S., Shaw, B., Curry, R., 2011. Continuous, array-based estimates of Atlantic Ocean heat transport at 26.5N. Journal of Climate 24, 2429–2449.
Johnson, G.C., 2008. Quantifying Antarctic bottom water and North Atlantic deep water volumes. Journal of Geophysical Research 113, C05027. http://dx.doi.org/10.1029/2007JC004477.
Johnson, G.C., Purkey, S.G., Toole, J.M., 2008. Reduced Antarctic meridional overturning circulation reaches the North Atlantic Ocean. Geophysical Research Letters 35, L22601. http://dx.doi.org/10.1029/2008GL035619.
Joyce, T., Hernández-Guerra, A., Smethie, W., 2001. Zonal circulation in the NW Atlantic and Caribbean from a meridional World Ocean Circulation Experiment hydrographic section at 66W. Journal of Geophysical Research – Oceans 106, 22095–22113.
Kanzow, T., Cunningham, S.A., Johns, W.E., Hirschi, J.J., Marotzke, J., Baringer, M.O., meinen, C.S., Chidichimo, M.P., Atkinson, C., Beal, L.M., Bryden, H., Colllins, J., 2010. Seasonal variability of the Atlantic meridional overturning circulation at 26.5°N. Journal of Climate 23, 5678–5698.
Katz, E.J., Garzoli, S.L., 1982. Response of the western equatorial Atlantic Ocean to an annual wind cycle. Journal of Marine Research 40, 307–327.
Koltermann, K., Sokov, A., Tereschenkov, V., Dobroliubov, S., Lorbacher, K., Sy, A., 1999. Decadal changes in the thermohaline circulation of the North Atlantic. Deep Sea Research Part II: Topical Studies in Oceanography 46, 109–138.
Lavín, A.M., Bryden, H.L., Parrilla, G., 2003. Mechanisms of heat, freshwater, oxygen and nutrient transports and budgets at 24.5N in the subtropical North Atlantic. Deep-Sea Research Part I 50, 1099–1128.
Lee, T.N., Johns, W., Schott, F., Zantopp, R., 1990. Western boundary current structure and variability east of Abaco, Bahamas at 26.5°N. Journal of Physical Oceanography 20, 446–466.
Lumpkin, R., Speer, K., 2003. Large-scale vertical and horizontal circulation in the North Atlantic Ocean. Journal of Physical Oceanography 33, 1902–1920.
Lux, M., Mercier, H., Arhan, M., 2001. Interhemispheric exchanges of mass and heat in the Atlantic Ocean in January–March 1993. Deep-Sea Research Part I 48, 605–638.
Macdonald, A., 1998. The global ocean circulation: a hydrographic estimate and regional analysis. Progress in Oceanography 41, 281–382.
Machín, F., Pelegrí, J.L., 2009. Northward penetration of Antarctic intermediate water off Northwest Africa. Journal of Physical Oceanography 39, 512–535.
Machín, F., Hernández-Guerra, A., Pelegrí, J.L., 2006. Mass fluxes in the Canary Basin. Progress in Oceanography 70, 416–447.
Machín, F., Pelegrí, J.L., Fraile-Nuez, E., Vélez-Belchí, P., López-Laatzen, F., Hernández-Guerra, A., 2010. Seasonal flow reversals of Intermediate Waters in the Canary Current System east of the Canary Islands. Journal of Physical Oceanography 40, 1902–1909.
Marcello, J., Hernández-Guerra, A., Eugenio, F., Fonte, A., 2011. Seasonal and temporal study of the northwest African upwelling system. International Journal of Remote Sensing 32, 1843–1859.
Martínez-Marrero, A., Rodríguez-Santana, A., Hernández-Guerra, A., Fraile-Nuez, E., López-Laatzen, F., Vélez-Belchí, P., Parrilla, G., 2008. Distribution of water masses and diapycnal mixing in the Cape Verde Frontal Zone. Geophysical Research Letters 35 (L07609), 2008G. http://dx.doi.org/10.1029/L033229.
McCartney, M., Bennett, S., Woodgate-Jones, M., 1991. Eastward flow through the Mid-Atlantic Ridge at 11N and its influence on the abyss of the eastern basin. Journal of Physical Oceanography 21, 1089–1121.
Meinen, C.S., Johns, W.E., Garzoli, S.L., van Sebille, E., Rayner, D., Kanzow, T., Baringer, M.O., 2013. Variability of the Deep Western Boundary Current at 26.5(N during 2004–2009). Deep Sea Research II 85, 154–168.
Nykjaer, L., Van Camp, L., 1994. Seasonal and interannual variability of coastal upwelling along northwest Africa and Portugal from 1981 to 1991. Journal of Geophysical Research 99, 14197–14207.
Orsi, A., Johnson, G., Bullister, J., 1999. Circulation, mixing, and production of Antarctic Bottom Water. Progress in Oceanography 43, 55–109.
Pacheco, M.M., Hernández-Guerra, A., 1999. Seasonal variability of recurrent phytoplankton pigment patterns in the Canary Islands area. International Journal of Remote Sensing 20, 1405–1418.
Parrilla, G., Lavín, A., Bryden, H., García, M., Millard, R., 1994. Rising temperatures in the subtropical North Atlantic Ocean over the past 35 years. Nature 369, 48–51.
Pastor, M.V., Peña-Izquierdo, J., Pelegrí, J.L., Marrero-Diaz, A., 2012. Meridional changes in water mass distributions off NW Africa during November 2007/2008. Ciencias Marinas 38, 223–244.
Pérez-Hernández, M.D., Hernández-Guerra, A., Fraile-Nuez, E., Comas-Rodríguez, I., Benítez-Barrios, V.M., Domínguez-Yanes, J.F., Vélez-Belchí, P., De Armas, D., 2013. The source of the Canary current in fall 2009. Journal of Geophysical Research – Oceans 118. http://dx.doi.org/10.1002/jgrc.20227.
Pickart, R.S., 1992. Water mass components of the North Atlantic deep western boundary current. Deep-Sea Research 39, 1553–1572.
Pollard, R., Pu, S., 1985. Structure and circulation of the upper Atlantic Ocean northeast of the Azores. Progress in Oceanography 14, 443–462.
Purkey, S.G., Johnson, G.C., 2012. Global contraction of Antarctic Bottom Water between the 1980s and 2000s. Journal of Climate 25, 5830–5844.
Richardson, P., Schmitz, W., 1993. Deep cross-equatorial flow in the Atlantic measured with Sofar floats. Journal of Geophysical Research – Oceans 98, 8371–8387.
Richardson, P., Bower, A., Zenk, W., 2000. A census of Meddies tracked by floats. Progress in Oceanography 45, 209–250.
Rintoul, S.R., Wunsch, C., 1991. Mass, heat, oxygen and nutrient fluxes and budgets in the North Atlantic Ocean. Deep-Sea Research 38, S355–S377.

Please cite this article in press as: Hernández-Guerra, A., et al. Meridional overturning transports at 7.5N and 24.5N in the Atlantic Ocean during 1992–93 and 2010–11. Prog. Oceanogr. (2014), http://dx.doi.org/10.1016/j.pocean.2014.08.016

Roach, A., Aagaard, K., Pease, C., Salo, S., Weingartner, T., Pavlov, V., Kulakov, M., 1995. Direct measurements of transport and water properties through the Bering Strait. Journal of Geophysical Research – Oceans 100, 18443–18457.

Roemmich, D., Wunsch, C., 1985. Two transatlantic sections: meridional circulation and heat flux in the subtropical North Atlantic Ocean. Deep-Sea Research 32, 619–664.

San Antolín Plaza, M.Á., Pelegrí, J.L., Machín, F.J., Benítez-Barrios, V., 2012. Inter-decadal changes in stratification and double diffusion in a transatlantic section along 7.5°N. Scientia Marina 76, 189–207.

Schmitz Jr., W.J., Richardson, P.L., 1991. On the sources of the Florida Current. Deep-Sea Research 38, S379–S409.

Schouten, M.W., Matano, Ricardo P., Strub, Ted P., 2005. A description of the seasonal cycle of the equatorial Atlantic from altimeter data. Deep Sea Research Part I: Oceanographic Research Papers 52 (3), 477–493. http://dx.doi.org/10.1016/j.dsr.2004.10.007.

Smeed, D.A., McCarthy, G.D., Cunningham, S.A., Frajka-Williams, E., Rayner, D., Johns, W.E., Meinen, C.S., Baringer, M.O., Moat, B.I., Duchez, A., Bryden, H.L., 2014. Observed decline of the Atlantic meridional overturning circulation 2004–2012. Ocean Science 10, 29–38.

Smethie, W.M., Fine, R.A., Putzka, A., Jones, E.P., 2000. Tracing the flow of North Atlantic Deep Water using chlorofluorocarbons. Journal of Geophysical Research: Oceans 105, 14297–14323.

Stramma, L., Schott, F., 1999. The mean flow field of the tropical Atlantic Ocean. Deep-Sea Research Part II 46, 279–303.

Talley, L., 2003. Shallow, intermediate, and deep overturning components of the global heat budget. Journal of Physical Oceanography 33, 530–560.

Talley, L.D., 2008. Freshwater transport estimates and the global overturning circulation: shallow, deep and throughflow components. Progress in Oceanography 78, 257–303.

Talley, L.D., McCartney, M.S., 1982. Distribution and circulation of Labrador Sea water. Journal of Physical Oceanography 12, 1189–1205.

Tomczak, M., Hughes, P., 1980. Three dimensional variability of water masses and currents in the Canary Current upwelling region. "Meteor" Forschungs-Ergebnisse A 21, 1–24.

Toole, J.M., Curry, R.G., Joyce, T.M., McCartney, M., Peña-Molino, B., 2011. Transport of the North Atlantic Deep Western Boundary Current about 39°N, 70°W: 2004–2008. Deep-Sea Research Part II 58, 1768–1780.

Tsuchiya, M., Talley, L.D., McCartney, M.S., 1992. An eastern Atlantic section from Iceland southward across the equator. Deep-Sea Research 39, 1885–1917.

van Aken, H.M., 2001. The hydrography of the mid-latitude Northeast Atlantic Ocean-Part III: The subducted thermocline water mass. Deep-Sea Research Part I 48, 237–267.

Wunsch, C., 1977. Determining the general circulation of the oceans: a preliminary discussion. Science 196, 871–875.

Wunsch, C., 1996. The Ocean Circulation Inverse Problem. Cambridge University Press.

Wunsch, C., 2005. The total meridional heat flux and its oceanic and atmospheric partition. Journal of Climate 18, 4374–4380.

Wunsch, C., Grant, B., 1982. Towards the general-circulation of the North-Atlantic Ocean. Progress in Oceanography 11, 1–59.

Zenk, W., Klein, B., Schröder, M., 1991. Cape Verde frontal zone. Deep-Sea Research 38, 505–530.

Zhang, D., Msadek, R., McPhaden, M.J., Delworth, T., 2011. Multidecadal variability of the North Brazil Current and its connection to the Atlantic meridional overturning circulation. Journal of Geophysical Research – Oceans 116, C04012. http://dx.doi.org/10.1029/2010JC006812.

Please cite this article in press as: Hernández-Guerra, A., et al. Meridional overturning transports at 7.5N and 24.5N in the Atlantic Ocean during 1992–93 and 2010–11. Prog. Oceanogr. (2014), http://dx.doi.org/10.1016/j.pocean.2014.08.016